LBL-31737
UC-800
Preprint

Lawrence Berkeley Laboratory
UNIVERSITY OF CALIFORNIA

EARTH SCIENCES DIVISION

Accepted for publication in abbreviated form in the journal *Fractals*

Fractal Surfaces: Measurements and Applications in the Earth Sciences

B.L. Cox and J.S.Y. Wang

April 1992

Prepared for the U.S. Department of Energy under Contract Number DE-AC03-76SF00098

REFERENCE COPY
Does Not
Circulate
Bldg. 50 Library.
LBL-31737
Copy 1

DISCLAIMER

This document was prepared as an account of work sponsored by the United States Government. While this document is believed to contain correct information, neither the United States Government nor any agency thereof, nor the Regents of the University of California, nor any of their employees, makes any warranty, express or implied, or assumes any legal responsibility for the accuracy, completeness, or usefulness of any information, apparatus, product, or process disclosed, or represents that its use would not infringe privately owned rights. Reference herein to any specific commercial product, process, or service by its trade name, trademark, manufacturer, or otherwise, does not necessarily constitute or imply its endorsement, recommendation, or favoring by the United States Government or any agency thereof, or the Regents of the University of California. The views and opinions of authors expressed herein do not necessarily state or reflect those of the United States Government or any agency thereof or the Regents of the University of California.

LBL-31737

FRACTAL SURFACES:

Measurement and Applications in the Earth Sciences

B. Lea Cox and J. S. Y. Wang

Earth Sciences Division
Lawrence Berkeley Laboratory
University of California
Berkeley, California 94720

April 1992

This work was supported by the Director, Office of Civilian Radioactive Waste Management, Yucca Mountain Site Characterization Project Office, Regulatory and Site Evaluation Division, under U.S. Department of Energy Contract No. DE-AC03-76SF00098.

Table of Contents

List of Figures v
List of Tables vii
Abstract ix

1.0. INTRODUCTION 1
- 1.1. Definitions 1
- 1.2. Fractals and Fractal Geometry 2
- 1.3. Self-Similarity 3
- 1.4. Self-Affinity 4
- 1.5. Fractal Dimension 6
- 1.6. Fractal Measure 7
- 1.7. Fractal Dimensional Increment 10

2.0. MEASUREMENT OF FRACTAL DIMENSION 10
- 2.1. Divider Method (Ruler Method) 10
- 2.2. Box Method 14
- 2.3. Triangle Method 16
- 2.4. Slit-Island Method 17
- 2.5. Power Spectral Method 19
- 2.6. Variogram Method 20
- 2.7. Distribution Method 21

3.0. APPLICATIONS IN THE EARTH SCIENCES 22
- 3.1. Map Data (Landscape Scale) 23
  - 3.1.1. Elevation Contours 23
  - 3.1.2. Channels (Caves and Streams) 24
  - 3.1.3. Fault Traces and Fault Networks 25
- 3.2. Fracture Surfaces 26
  - 3.2.1. Rock Fractures in the Field and in Hand Specimens 26
  - 3.2.2. Fractures in the Laboratory 28
- 3.3. Porous Aggregates 30
  - 3.3.1. Pore Geometry 30
  - 3.3.2. Flow and Transport 30
  - 3.3.3. Spatial Variability 32
- 3.4. Microscopic Surface Phenomena 33
  - 3.4.1. Surface Adsorption 34

3.4.2. Particle Aggregation 35
3.4.3. Erosion and Chemical Dissolution 35
4.0. DISCUSSION OF MEASUREMENT METHODS 36
5.0. DISCUSSION OF APPLICATIONS 40
6.0. CONCLUSIONS 41
7.0. ACKNOWLEDGEMENTS 43
8.0. REFERENCES 43

List of Figures

		Page
Figure 1.	Congruent, similar and affine shapes	3
Figure 2.	Examples of deterministic fractal construction	5
Figure 3.	Exact versus statistical self-similarity	6
Figure 4.	Fractal dimension of self-similar shapes	8
Figure 5.	Profiles with different fractal dimensions	9
Figure 6.	Divider (ruler) method	13
Figure 7.	Box method	15
Figure 8.	Triangle method	17
Figure 9.	Slit-island method	18
Figure 10.	Power spectral method	20
Figure 11.	Variogram method	21
Figure 12.	Distribution method	22
Figure 13.	Surface and mass fractals measurement	34
Figure 14.	Overhangs	39

List of Tables

		Page
Table 1	Fractal measurements from different applications	11
Table 2	Fractal measurements by seven methods: formulae	12
Table 3	Comparison of fractal measurements	27

Abstract

Earth scientists have applied different methods to the measurement of fractal dimension of surfaces. The divider, box, triangle, slit-island, power spectral, variogram and distribution methods differ in the procedures to analyze the fractal dimension of spatial distributions of data. However, fractal dimension may vary systematically with measurement method. In studies which used more than one technique to measure the fractal dimension of a surface, the power spectral method tended to yield the largest fractal dimension, while the divider method tended to give the smallest fractal dimension. The box, triangle, and slit-island methods were intermediate. Possible reasons for these differences are discussed. Several common problems to all of the methods need to be considered, such as the remainder problem, curve-fitting, orientation of the measurement plane, size and direction of the sample. These practical difficulties in fractal dimension determination are not restricted to topographic surfaces, but also apply in general to manifestations of spatial distributions of other measurable quantities. Fractal measurements have been applied to many problems in the earth sciences, at a wide range of spatial scales. These include map data of topography; fault traces and fracture networks; fracture surfaces of natural rocks, both in the field and at laboratory scales; metal surfaces; porous aggregate geometry; flow and transport through heterogeneous systems; and various microscopic surface phenomena associated with adsorption, aggregation, erosion and chemical dissolution. These applications of fractal measurement fall into a few general categories: characterization of surface geometry in order to determine underlying structures; correlation of surface geometry with formation or degradative processes; use of fractal geometry to disentangle multiple processes and the scales over which they are dominant; use of fractal geometry to interpolate or extrapolate data; and the use of fractal geometry in empirical equations in order to estimate difficult-to-measure parameters. The usefulness and limitations of fractal geometry in earth science applications are discussed.

1.0. INTRODUCTION

Fractal theory has been applied in many earth science disciplines, including geology, geochemistry, geophysics, geomorphology, geography, hydrology, and soil sciences, and at a wide range of spatial scales, from mega-scale observations of plate boundaries such as the San Andreas Fault, to micro-scale studies of pore and molecular structures. The fractal dimension is one of the main parameters of fractal geometry (Mandelbrot, 1982). There are different definitions of the fractal dimension and several techniques have been developed for measuring fractal dimensions of surfaces. One objective of this report is to review the methods which have been used in earth sciences to measure fractal dimensions of surfaces, and to compare the results of measurements made of the same surface by different methods. We also evaluate the problems involved in the use of different methods, and discuss the usefulness of fractal measurements, given the error and variability of measurements for a given surface.

In addition to the different methods, we review applications of the fractal theory to research in the earth sciences, and discuss some of the problems with these applications. We would like to identify where more work is needed in both the theory and application of fractals to natural surfaces in the earth sciences. We focus on the applications of fractal geometry to nearly-planar surfaces (with Euclidean or topological dimension $D_T = 2$). General reviews of the use of fractal geometry to pointed ($D_T = 0$), linear ($D_T = 1$), planar ($D_T = 2$) and volumetric ($D_T = 3$) subjects can be found in Avnir (1989); Falconer (1990); Jullien and Botet (1987); Mandelbrot (1982); Martin and Hurd (1987); Meakin (1991); Peitgen and Saupe (1988); and Turcotte (1989). We focus on the studies of natural surfaces and not on simulated surfaces. A systematic comparison of different algorithms for simulated fractal surfaces will be the subject of a subsequent report.

This review was motivated by our interests in quantifying experimentally determined aperture distributions of natural fractures bounded by rough rock surfaces (Cox et al., 1990) and in studying theoretically the use of fractal geometry and geostatistical models to represent rock fractures (Wang et al., 1988). When we tried to use different models to represent rough surfaces and used different methods to determine the fractal dimension and other geostatistical correlation structures, we found out that the determination of the fractal dimension of a surface was not trivial. A review of the literature shows that similar difficulties have been encountered by many other researchers applying fractal geometry to natural surfaces.

1.1. Definitions

We start with definitions of different terminology of fractal geometry. Fractals and fractal geometry are general concepts based on self-similarity and self-affinity. Fractal dimension D is a numerical parameter obtained from analyzing the data of physical measurement. While the topological dimension D_T is always an integer, the fractal dimension D need not be an integer.

1.2. Fractals and Fractal Geometry

The word "fractal" and the systematic study of fractal geometry began with Mandelbrot's research at IBM in the 1970's, culminating in his book "Les Objets Fractals" (1975), followed in 1982 by "The Fractal Geometry of Nature." Fractal geometry provides a framework for the study of some of the mathematical sets or functions which are considered "pathological;" that is, those which are not sufficiently smooth or regular to be studied using the methods of classical Euclidean geometry and calculus. This new approach to geometry opened up a field which is very interdisciplinary, with applications for artists, natural scientists, physical scientists, film-makers, mathematicians and computer scientists. It is interesting that after more than a decade of research, systems of classical dimension of 1, 2, or 3 are now considered by some researchers as degenerate (Pfeifer and Obert, 1989), rather than fractal geometry being considered pathological.

Mandelbrot selected the word fractal because linguistically it describes an irregular fragment or shape. Yet, one can also use fractal dimension to describe a smooth, undulating curve. There is no very satisfactory definition of what is meant by the word (adjective or noun) "fractal," because it describes an approach to shape description over scale changes, but is not a concrete object. One can generate fractal shapes and one can measure fractal dimension of various shapes, but the definition of what makes an object fractal is somewhat fuzzy.

> "A fractal is by definition a set for which the Hausdorff Besicovitch dimension strictly exceeds the topological dimension" (Mandelbrot, 1982, p. 15).

The Hausdorff-Besicovitch dimension is a self-similar or fractal dimension and is discussed in section 1.4. This definition excludes many sets that ought to be considered fractal (Falconer, 1990). Falconer (1990, p. xx) states that

> "My personal feeling is that the definition of a 'fractal' should be regarded in the same way as the biologist regards the definition of 'life'. There is no hard and fast definition, but just a list of properties characteristic of a living thing... ."

Some of the characteristics which fractals usually share are that they have detail at arbitrarily small scales, they are too irregular to be described in traditional geometric terminology; they have some form of self-similarity; they usually can be defined by some simple, recursive algorithm; and the fractal dimension, defined in some way, is usually greater than the topological dimension (Falconer, 1990). The topological dimension is the whole number which is generally associated with a geometric object (e.g. the topological dimension of a line is 1, of a plane or surface is 2, and of a volume is 3). The fractal dimension is used to describe "rough" geometric objects, such as a squiggly line, a bumpy surface, or a porous volume, and includes non-integers as well as integers. Every set with a noninteger fractal dimension is a fractal. However, a fractal may have an integer fractal dimension, such as the trail of Brownian motion with a topological dimension $D_T = 1$ and a fractal dimension $D = 2$ (Mandelbrot, 1982, p. 12).

1.3. Self-Similarity

The best way to introduce the notion of self-similarity is to start with the concept of congruence, proceed then to similarity, and finally to self-similarity. Congruence between two shapes means that they are exactly the same, allowing only differences in orientation and polarity (Figure 1a,b). Given two congruent shapes, if one of these shapes shrinks or expands uniformly, while the other remains undeformed, the two shapes lose their congruence and become similar (Figure 1c). The degree of shrinkage or expansion is quantified by a scaling factor.

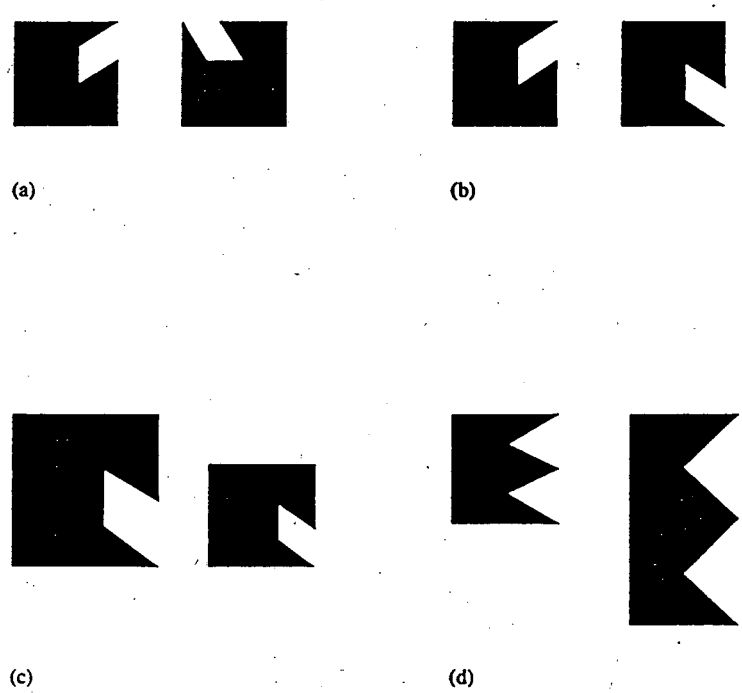

Figure 1. Congruent (a,b) similar (c) and affine (d) shapes. After Falconer, 1990.

One can apply the same scaling factor repeatedly and generate a set of similar shapes. The set of all possible shapes related by a single scaling factor is a self-similar set. If we look at a shape in a self-similar set at a different scale, we will see the same repetitive shape or pattern. This self-similarity may be exact (deterministic) or statistical. Deterministic self-similarity indicates the repetition of a pattern exactly over many levels of detail. Statistical self-similarity indicates that the repetition of a pattern follows a random distribution or a random rule.

Five examples of deterministic fractals (the middle third Cantor, the von Koch, the Sierpinski gasket, the Cantor dust and the Julia set) are shown in Figure 2. The middle third Cantor set is constructed by repeated removal of the middle third intervals of a set of parallel lines. The von

Koch curve is constructed by recursively replacing the middle third of a line segment by the other two sides of an equilateral triangle based on the removed segment. The Sierpinski gasket is constructed by repeated removal of inverted equilateral triangles which bisect the sides of a larger equilateral triangle. If the shapes are squares instead of triangles, this would be a Sierpinski carpet, a two-dimensional analogue of the middle third Cantor set. A Cantor dust is constructed by recursively dividing squares into four smaller squares located at the corners, each of which is 1/16 of the original square. The Julia set is constructed from a single quadratic function $f(z) = z^2 + c$. While the other fractals in Figure 2 are strictly self-similar, the Julia set is quasi-self-similar requiring small regions to be both magnified and distorted to correspond to larger regions (Falconer, 1990).

The deterministic self-similarity shown by the fractal constructions in Figure 2 is not the same as the self-similarity of natural surfaces. Natural surfaces usually have statistical rather than exact self-similarity. For example, the outline of a coastline, viewed at different scales, will be similar in an average sense (statistically) at different scales, but the correspondence is not exact. Figure 3 contrasts the generation of an exact with a statistically self-similar von Koch curve (Falconer, 1990). In Figure 3b, the von Koch curve was randomized by tossing a coin to determine whether to position the new triangular segment pointing in or out of the line segment. Other deterministic fractals can be randomized in various ways. For example, the construction of the Sierpinski gasket shown in Figure 2 could be randomized by using distorted triangles whose orientations were determined by a random process. In addition to direction and orientation, one can also treat the scaling factor as a random variable, with given mean and distributions, to construct random fractal patterns. These fractal patterns may visually resemble natural landscape topography.

1.4. Self-Affinity

A linear non-singular transformation of a shape results in a new shape which is affine in relation to the original shape The distortion need not be the same in all coordinate directions. For example, starting with two congruent shapes which look like the left hand shape in Figure 1d, we can transform one of these shapes by stretching it in the vertical direction so that it looks like the right hand shape in Figure 1d. These two shapes are no longer similar, but are affine. A self-affine set could be constructed by iterating a pattern such that the scaling factors are different along different coordinate axes. Natural phenomena, such as landscapes or fracture surfaces, are more likely to be self-affine, rather than self-similar, because processes producing the topography vary in different directions. For example, basin and range topography typical of Nevada and southeastern California, consists of horst and graben structure (uplifted mountain ranges adjacent to downfaulted basins), along a northeasterly trend. The pattern of a profile traced along the northeasterly trend would be very different than that measured perpendicular to the trend. Superimposed on these strong tectonic geometric patterns are the cumulative modifications by climatic factors due to wind, water, and gravitational forces. The patterns created by these climatic forces will scale differently, both spatially and temporally, from the pattern due to the tectonic processes. If there is a statistical scaling relationship to the patterns, this relationship will most

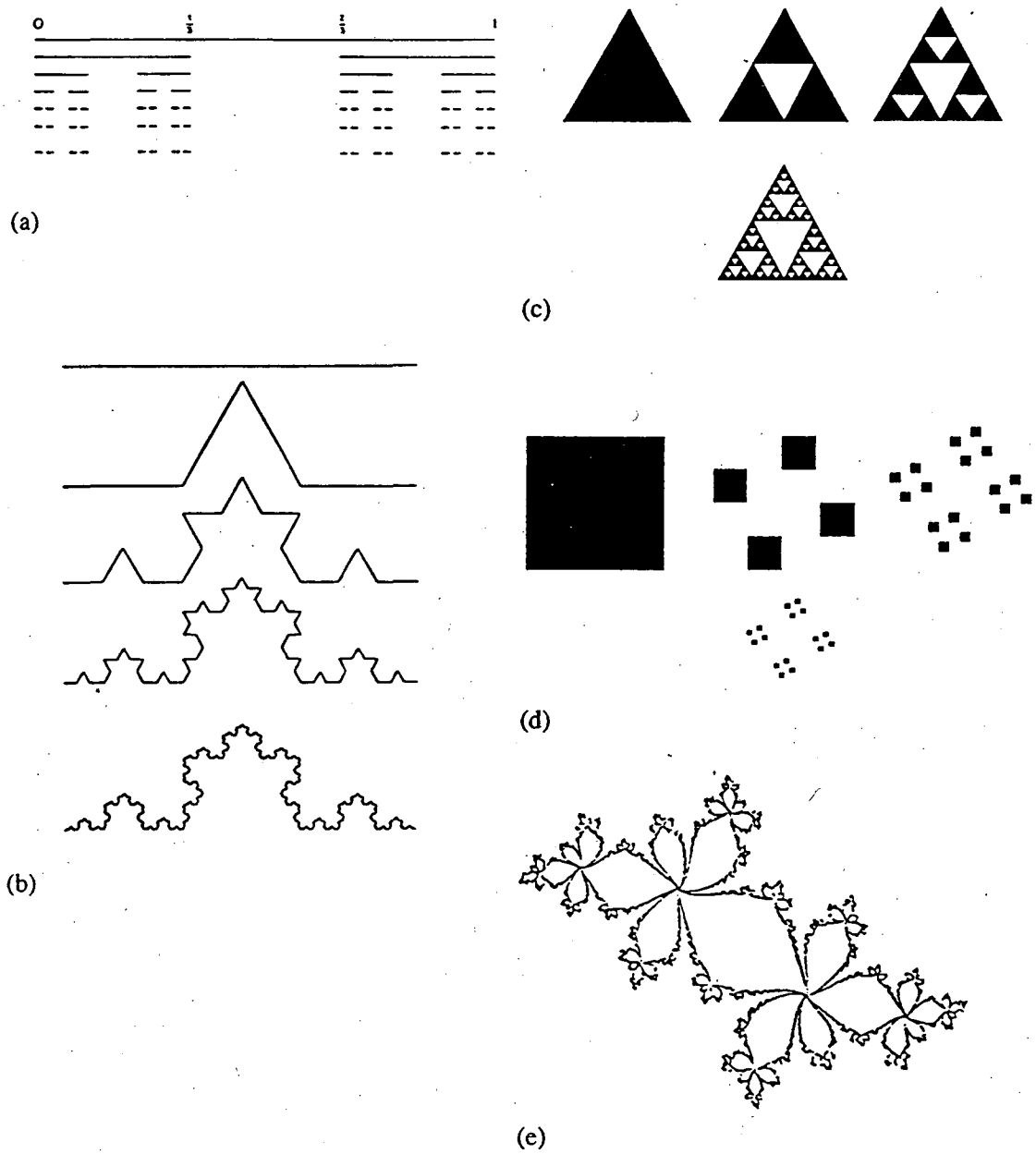

Figure 2. Examples of deterministic fractal construction: middle third Cantor set (a); von Koch curve (b); Sierpinski gasket (c); Cantor dust (d); Julia set (e). From Falconer, 1990.

likely differ depending on whether the pattern is measured along horizontal cuts (contours) or vertical cuts (profiles). Thus, these landscape or geomorphic surfaces preserve a scaling relationship only if one considers the vertical and horizontal orientations separately.

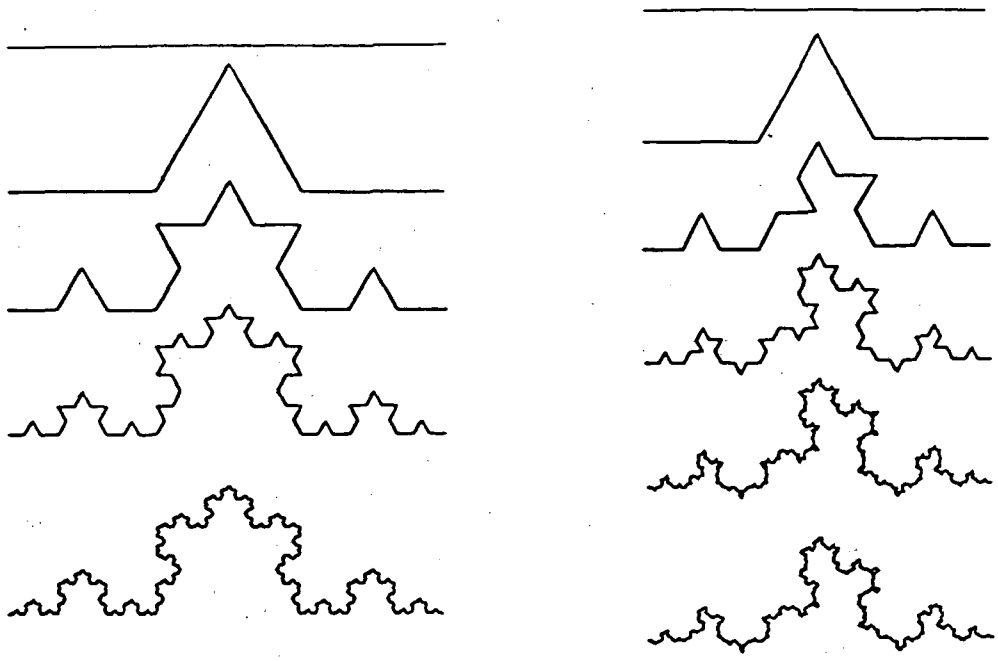

(a) (b)

Figure 3. Exact(a) versus statistical (b) self similarity. From Falconer, 1990.

1.5. Fractal Dimension

In general, fractal dimension provides a description of how the space is occupied by a particular curve or shape. This shape or curve may be a physical object or a mathematical model to describe the object. Figure 4(a) illustrates the traditional use of integer spatial dimensions (Euclidean dimensions) for the scaling of objects, i.e. lines, planes and volumes, and Figure 4(b) the generalization of the concepts of dimension to fractal patterns with non-integer dimensions. By dividing a straight line segment of unit length $L = 1$ into N parts, each of length r, $N_r = 1$. Dividing a square and a cube in a similar manner yields $Nr^2 = 1$ and $Nr^3 = 1$, respectively. The exponent of r is the topological dimension D_T (= 1 for a line, 2 for a surface, and 3 for a volume). For more general self-similar shapes, we have $Nr^D = 1$, where D is the fractal or similarity (Hausdorff-Besicovitch) dimension of that object or curve and

$$D = \log(N)/\log(1/r) = -\log(N)/\log(r).$$

D is usually greater than the topological dimension for a fractal object.

The von Koch curve shown on Figure 2 will thus have a similarity dimension of $-\log 4/\log 1/3 = \log 4/\log 3 = 1.262$. That is, there are four copies of the pattern over a length scale of 1, each copy taking up 1/3 of the length. The Cantor set has a similarity dimension of log 2/log 3 = 0.631. The fractal dimension would be identical to this similarity dimension for these strictly self-similar fractal sets.

Mathematically, different similarity dimensions can be defined according to various rigorous definitions in set theory or other mathematical theories. For example, the Hausdorff-Besicovitch dimension is defined by set theory based on how a set is covered by specified intervals. The box-counting or box dimension, also known as Kolmogorov entropy or entropy dimension, is defined in the following manner (Falconer, 1990):

> Let F be any non-empty bounded subset of R^n and let $N_r(F)$ be the smallest number of sets of diameter at most r which can cover F. The lower and upper box-counting dimensions of F respectively are defined as the limit is approached from below or above, as

$$D_l = \lim_{r \to 0} \frac{\log N_r(F)}{-\log r}$$

While the box dimension is different mathematically from the Hausdorff-Besicovitch dimension, they are essentially equivalent in practice.

We are mainly interested in the practical quantification of fractal or similarity dimensions for natural patterns and do not attempt to distinguish the mathematical differences in the definitions of different dimensions. However, some of the confusion and ambiguity in quantifying a fractal dimension could be related to differences in the procedures (thus definitions) among different dimensions. There are many different ways of defining fractal dimension, depending on the nature of the system being described and the characteristics of the model being used to represent the system. More attention needs to be given to the problem of linking the mathematical definitions with the practical applications.

1.6. Fractal Measure

The length of a fractal curve is

$$\text{Length} = rN(r)$$

where r is the length of the measuring device, and N is the number of these lengths needed to traverse the line from an initial point to an end point. If the self-similarity of a fractal curve is not exact, but statistical, then N(r) varies, on the average, as $1/(r^D)$ and length is proportional to $1/(r^{D-1})$. If we treat r as the length of a measurement interval (ruler) moving along the curve, the length of the coastline will vary with the change in the size of the ruler. The total curve length increases as the ruler length decreases, and the fractal dimension characterizes this rate of change in length with change in scale (ruler length).

The fractal dimension characterizes the scaling and similarity property "within" a curve or an object but cannot distinguish the overall topography. For example, the von Koch curves shown in Figure 3 are convex upwards, similar to a pattern of positive relief such as a mountain range. If this profile were turned upside-down it would still have the same fractal dimension, yet it would now be a landscape of negative relief, with deep valleys. In the description of fractal geometry, one cannot distinguish these two very different topographies.

(a) **Integer Objects**

1-D N line segments; ratio $r=1/N$; $Nr^1=1$.

2-D N plane sections; ratio $r=\frac{1}{N^{\frac{1}{2}}}$; $Nr^2=1$.

3-D N volumes; ratio $r=\frac{1}{N^{\frac{1}{3}}}$; $Nr^3=1$.

Generalize:
For an object of N parts, scaled by a ratio r from the whole,

$$Nr^D=1$$

$$D=\frac{LogN}{Log\frac{1}{r}}$$

For integer object, $D=D_t$

(b) **Non-Integer Lines**

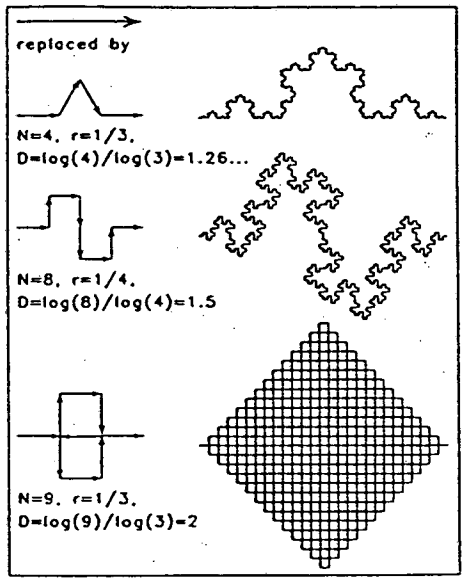

Figure 4. Fractal dimension of self-similar shapes: integer dimensional figures (a); non-integer fracture figures (b). From Peitgen and Saupe, 1988.

The fractal dimension measures the relative amounts of detail or "roughness" occurring at different scales. Surfaces with a larger fractal dimension appear "rougher" and are richer in detail. Figure 5 shows three profiles with different fractal dimensions, demonstrating the visual appearance of a positive correlation between roughness and fractal dimension. Yet, roughness and fractal dimension are not synonymous. Roughess is generally measured as the average variation about the mean value, and is not related to the scale or changes in scale of measurement. Fractal dimension is used to quantify the variation of the length or area or volume with changes in the scale of measurement interval. Fractal dimension is an intensive property while roughness is not (Avnir et al., 1985). (An intensive property, such as temperature, pressure, or fractal dimension, does not depend on the amount of material present, while an extensive property, such as volume and roughness, does depend on the amount of substance in the system). One of the objectives of our review of the fractal geometry of rough rock surfaces is to examine the relationship, or correlation, if existing, between roughness and fractal dimension.

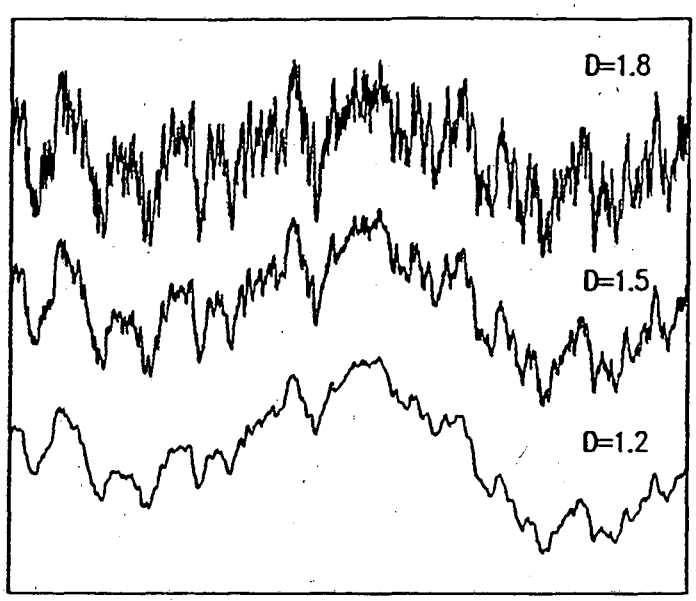

Figure 5. Profiles with different fractal dimensions. Profiles are samples of fractional Brownian motion. From Peitgen and Saupe, 1988.

1.7. Fractal Dimensional Increment

In several papers the terminology "fractal dimensional increment" is used (see for example, Mandelbrot et al., 1984). This is defined as the increment which exceeds the topological or Euclidean dimension. We use the fractal dimensional increment when we discuss and compare measurements taken from profiles and measurements taken from contours to represent a surface. The fractal dimension of a non-planar surface will be greater than 2 and less than 3. If this dimension is 2.4, then the fractal dimension of its coastline would be 1.4 and the fractal dimensional increment D_{inc} is 0.4 (Peitgen and Saupe, 1988). The quantity $H = 1 - D_{inc}$ is the Hurst exponent frequently used in describing fractional Brownian motion.

2.0. MEASUREMENT OF FRACTAL DIMENSION

Numerous measurements of fractal dimensions on natural surfaces appeared in the published literature soon after Mandelbrot's two volumes (1977, 1982). We have selected references which demonstrate the use of different measurement methods as well as the application of these methods to different types of problems related to earth sciences and natural surfaces. There are basically seven techniques for measuring fractal dimension of natural surfaces. Four of these methods apply directly to a simple geometrical pattern: 1) the divider (or ruler) method, 2) the box method, 3) the triangle method and 4) the slit-island method. These methods involve the direct measurement of the length of a contour, boundary or profile, and/or the measurement of an area. The slit-island method differs from the first three methods in that it requires the measurement of a population of geometrical patterns, rather than a single pattern. The other three methods apply to a functional representation of variability. The 5) power spectral method uses integral transform to measure a boundary or profile. The other two methods are statistical measurement methods: 6) the variogram method, and 7) the size distribution method. We include both geometric and functional representation methods, because we are interested in the fractal dimension of spatial distributions of data over a two-dimensional plane, not just physical topography.

Table 1 lists some of the articles cited in this report which correspond to each of the seven methods. The application for which the measurement was made, as well as the fractal dimension measured, are also shown in this table. The fractal dimension shown on the table is the fractal dimensional increment, defined above as the difference between the fractal dimension and the topological or Euclidean dimension. Table 2 summarizes the plotting parameters and formulae for computing D for each of the seven methods.

2.1. Divider Method (Ruler Method)

The divider method is the oldest method of determining the fractal dimension. Its use as a measurement technique (Richardson, 1961) predates the invention of the word "fractal." The basic method involves measuring the length of a curve either at different resolutions, or with different sizes of measuring stick (ruler). This curve could be a topographic profile (Gilbert, 1989), a contour (Norton and Sorenson, 1989), the silhouette of a particle (Akbarieh and Tawashi, 1989), or a signal from time series data (Langford et al., 1989). Other names for this technique are the

Table 1. Fractal Measurements from Different Applications

Method	Reference	Application	F.D.Increment
Divider	Norton et al.,1989	Granite Mountain Profile	.15 to .28
Divider	Snow,1989	Stream Channels	.04 to .38
Divider	Aviles et al.,1987	San Andreas Fault Trace	.0008 to .0191
Divider	Brown,1987	Rock Fracture Surface	.50
Divider	Carr,1989	Rock Fracture Surface	.0000 to .0315
Divider	Miller et al.,1990	Rock Fracture Surface	.058 to .261
Divider	Underwood and Banerji,1986	Steel Fracture	.351 to .512
Divider	Akbarieh et al., 1989	Erosion of Ca-oxal.crystals	.025 to .106
Divider	Kaye,1986	Carbon particles	.32
Divider	Kaye,1986	unpolished Cu surface	.47
Divider	Kaye,1986	polished Cu surface	.00
Box	Barton and Larsen,1985	Rock Fracture Network	.12 to .16
Box	LaPointe,1988	Rock Fracture Network	.37 to .69
Box	Miller et al.,1990	Rock Fracture Profile	.041 to .159
Box	Hirata,1989	Japan Fault Network	.05 to .60
Box	Okuba et al.,1987	San Andreas Fault Trace	.2 to .4
Box	Sreenivasan et al.,1989	Turbulent Flow Interface	.35
Box	Langford et al.,1989	Epoxy Fracture	.35
Box	Langford et al.,1989	MgO Fracture	.16
Triangle	Denley,1990	Gold Film Surface	.04 to .46
Slit-Island	Mecholsky et al.,1988	Chert Fracture	.15 to .32
Slit-Island	Schlueter et al.,1991	Sandstone Pores	.31 to .40
Slit-Island	Schlueter et al.,1991	Limestone Pores	.20
Slit-Island	Huang et al.,1990	Steel Fracture Surface(lakes)	.20 to .30
Slit-Island	Huang et al.,1990	Steel Fracture Surface(islands)	.33 to .40
Slit-Island	Mandelbrot et al.,1984	Steel Fracture Surface	.28
Slit-Island	Pande et al.,1987	Titanium Fracture Surface	.32
Slit-Island	Langford et al.,1989	Epoxy Fracture Surface	.32
Spectral	Gilbert,1988	Sierra Nevada Topography	(-).835 to .471
Spectral	Brown et al.,1985	Rock Fracture	.26 to .68
Spectral	Carr,1989	Rock Fracture	(-).880 to .467
Spectral	Miller et al.,1990	Rock Fracture	.124 to .383
Spectral	Mandelbrot et al.,1984	Steel Fracture	.26
Spectral	Langford et al.,1989	Photon emission from epoxy fracture	.45
Variogram	Burrough,1989	Soil pH variation	.6 to .8
Variogram	Burrough,1989	Soil Na variation	.7 to .9
Variogram	Burrough,1989	Soil Elec.Resist.Variation	.4 to .6
Variogram	Armstrong,1986	Soil Microtopography	.64 to .90
Distribution	Curl,1986	Cave Length, Volume	.4, .8
Distribution	Krohn,1988	Sandstone Pores	.49 to .89
Distribution	Katz and Thompson,1985	Sandstone Pores	.57 to .87
Distribution	Krohn,1988	Carbonate and Shale Pores	.27 to .75
Distribution	Avnir et al.,1984	Carbonate particles	.01 to .97
Distribution	Avnir et al.,1984	Soil Particles	.43 to .99

Table 2. Fractal Measurements by 7 methods: Formulae

Method	Log X-axis	Log Y-axis	Formula for D
Divider	Ruler Length	Sum of Ruler Lengths	D = 1-slope
Box	1/Box Side	Total # of Boxes	D = slope
Triangle	Grid Spacing	Total Area/minimum area	D = 2-slope
Slit Island	Perimeter	Area	D = 2/slope
Spectral	Frequency	Spectral Density	D = (5-slope)/2
Variogram	Distance between Measurements,(h)	semi-variance,v(h)	D=(4-slope)/2
Distribution	Number above cutoff size	area	D=2(slope)

yardstick method or the structured walk technique (Kaye, 1989).

The essential characteristics of this method are illustrated in Figure 6a. First, walk the ruler or caliper along the profile and record the length (which equals the number of ruler lengths times the size of the ruler). Next, change the length of the ruler and repeat the measurement. Repeat this process several times, each time with a different ruler length. Then plot the log of the curve length versus the log of the ruler length, and if the data plot along a straight line, the profile has fractal geometry. (This plot is sometimes called a "Richardson plot"). Determine the slope of the line which best fits the data, and compute the fractal dimension from this slope. As we noted earlier in section 1.5, the length is proportional to r^{1-D}. The fractal dimension D equals one minus the slope.

There are several variations on how one might discretize this measurement. When one measures the contour or profile, the usual method is to start at some initial point along the curve, and moving along the curve from the initial point, measure equal intervals along the curve itself (Figure 6a). A remainder which doesn't fill the last ruler usually exists, and some means of handling this remainder must be devised. An alternative method for profiles is to project vertical lines at equal intervals along a baseline up to the profile (Figure 6b). Then, connect the intersections of the vertical lines, and measure the distances between these intersections. This second approach will not result in a remainder. These two approaches, that of measuring equal intervals along a curve, and that of measuring equal intervals along a baseline, may give different fractal dimensions. A third approach, used with digitized data (Clark, 1986), is shown on Figure 6c. Here, the interval or ruler is defined by a specified number of grid points. This number of points consists of both horizontal and vertical components, so that the length of each step will be different. An average step length is obtained by dividing the total length by the number of steps. This process is repeated at different resolutions. The results are then plotted on a log-log scale, with the average step length on the x-axis and the total length on the y-axis, and the slope is used to calculate the fractal dimension.

Two image analysis techniques have been used to determine the fractal dimension (Kaye, 1989). One uses a scan line inspection system to analyze television images of the boundary. The

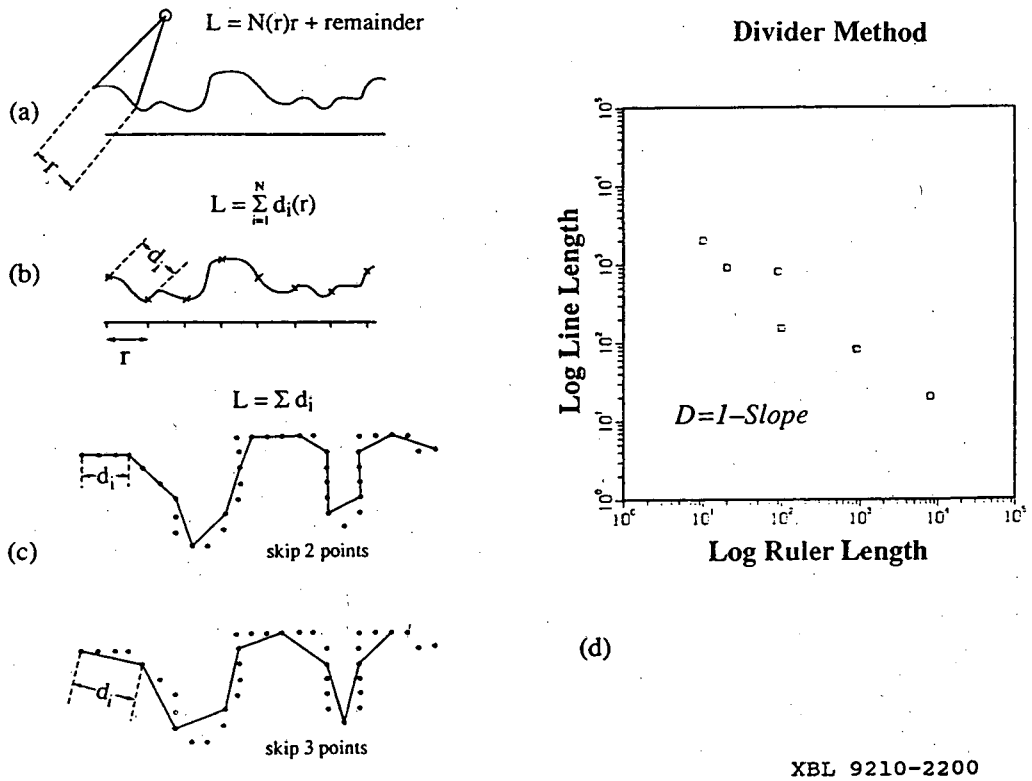

Figure 6. Divider (ruler) method: caliper or divider applied to surface of profile (a); modified divider where straight line length between divisions along base are measured (b); digitized ruler method using point counting (c) (Clark, 1986); example of plotted measurements where D = 1 - slope (d).

distance between the scan lines is the resolution parameter. The pixel coordinates of the intercepts between the image and the scan lines determine the perimeter of the boundary. This is repeated over a range of scan line spacings to generate a Richardson plot. Another image technique is based on adding pixels to the image and making a boundary appear as a ribbon. This is known as the dilation-erosion procedure. The area of the ribbon is evaluated by the image analyzer and the perimeter is estimated for a given dilation level from dividing the area by the thickness of the ribbon. These two image techniques are variations of the divider method (Kaye, 1989).

When determining the fractal dimension of surfaces, a series of profiles across the surface need to be measured. The data for all of the profiles can be plotted on one graph to determine the

fractal dimension. An alternative is to make individual plots of profiles, and the fractal dimension of the surface will then be related to the average of the fractal dimensions of the individual profiles. Since the fractal dimension of a surface should lie between 2 and 3, and the fractal dimension from a contour or profile will range between 1 and 2, researchers add 1 to the average fractal dimension obtained from the profiles.

For natural surfaces, the divider method often gives fractal dimensions near two (Aviles et al., 1987; Brown, 1987), which would indicate a smooth planar surface. Brown states that one explanation for this is that the surface is self-affine, and that the horizontal resolution is too great to detect the surface irregularity. Crossover length is the maximum scale at which irregularity is observable, and if the horizontal resolution is greater than the crossover length for self-affine surfaces, the surface will appear flat. Brown incrementally magnified the profile height (the vertical scale) repeatedly until a stable fractal dimension (a constant slope) was obtained. In other words, by increasing the vertical scale, the slope of the log-log plot kept changing until he reached a vertical scale beyond which the slope didn't change. This is based on the assumption that the magnification can equalize the horizontal and vertical scaling factors and transform a self-affine surface into a self-similar surface.

Before performing the fractal measurement by the divider method, it would be very useful to know whether or not the surface was self-affine. Matsushita and Ouchi (1989) designed a method to analyze self-affinity in topographic data. A fixed ruler scale was used to measure the length between many pairs of points on a profile or a contour. For each pair, the coordinates of all of the measurement points of the ruler are used to calculate two standard deviations in the two coordinate directions (x and y for contours, x and z for profiles). The standard deviation (for x and y or for x and z) versus length for many pairs of points are plotted on a log-log scale. The slopes of these two lines yields the self-affine exponents, v_x and v_y, or v_x and v_z. If v_x and v_y are the same, then the curve is self-similar, and $H = v_x = v_y$, and D_{inc} (the fractal dimensional increment) $= 1-H$. If they are different, then the curve is self-affine.

2.2. Box Method

The box method uses boxes to measure the length of a curve, or the density of lines or points over an area (Mandelbrot, 1982; Hirata, 1989; Barton and Larsen, 1985; La Pointe, 1988; Sreenivasan et al., 1989). The curve may be either a profile measured across a surface, or contours resulting from a horizontal slice taken through the surface. The curve is covered with square boxes as shown in Figure 7a. The size of the box is the length of the square. The number of same size boxes needed to cover the line is counted. This is repeated for a series of different sized boxes. The results are then plotted as the number of boxes (y-axis) versus 1 /(box size) on a log-log plot (Figure 7). The fractal D is equal to the slope of the plot. A variation on this method is to use circles instead of squares (Okuba et al., 1987), where the diameter of the circle is equivalent to the box size.

There are different ways of applying the box method. Some of these methods are presented in Goodchild (1980). The box method can be easily implemented with a computer algorithm by

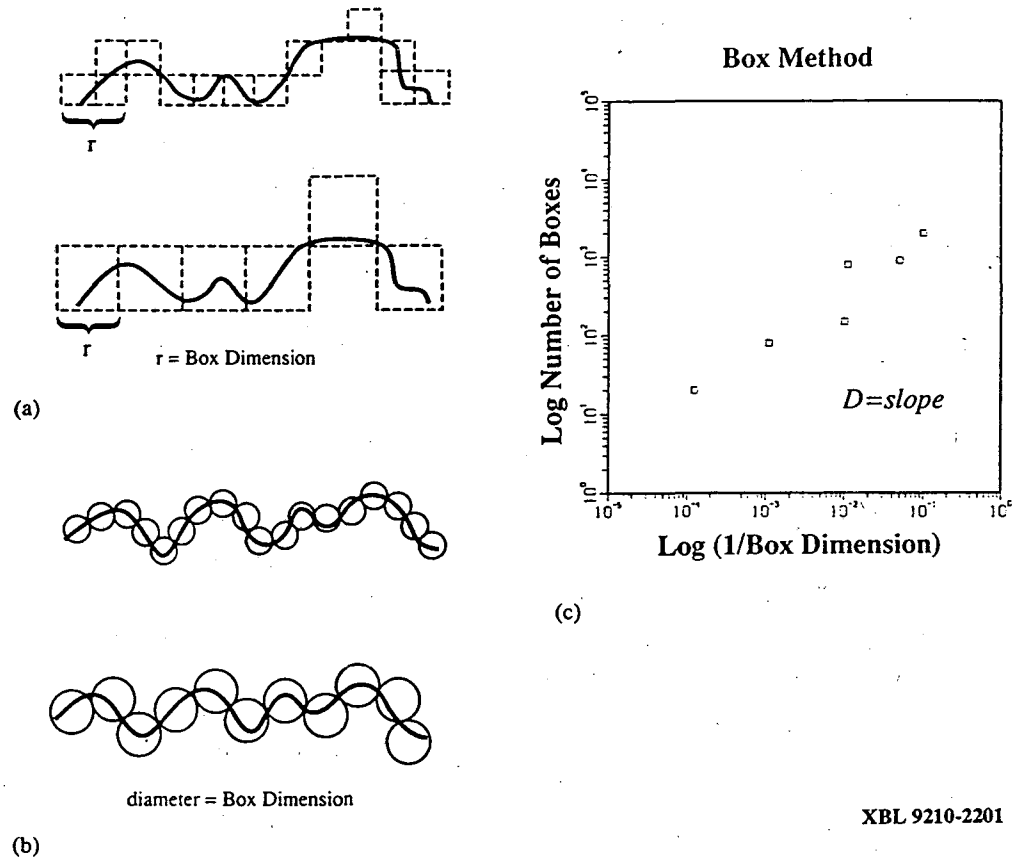

Figure 7. Box method: profile is covered with square boxes (a); with circles (b); example of data plot with D = slope.

defining the boxes with a rectangular grid. One can then count the number of intersections of the line with the boxes (grid elements or tiles), or alternatively, the number of boxes intersected by the line. When using a computer, one can start with the finest resolution image and then mathematically combine tiles into larger, lower resolution images, a procedure called "mosaic amalgamation" (Kaye, 1989). The box method can be used to analyze areas within curves as well as the curve itself. One can apply the centroid rule where the centroid of the box has to lie in the region of interest (not on the other side of the line) for the box to be counted. One can also apply the "majority rule," where a box is counted if more than half of its area lies within the region of interest.

Map interpretation requires the estimation of lengths of boundary lines and of areas defined by the boundaries. Goodchild (1980) showed how these map measurement problems are related to fractal dimension. He generated surfaces of prescribed fractal dimension, then covered the surfaces with boxes, and classified the boxes as to whether the centroid lay above or below the contour value. The error of the method could then be estimated and related to the fractal dimension. By understanding this relationship, the fractal dimension could then be used to estimate the optimal grid size for use in geographic and geomorphic studies. This optimization is based on a tradeoff between computational effort and expected error. The error decreases while the computational effort increases as box size decreases.

The application of the box method to the measurement of the fractal dimension of the surface, rather than to a single curve, requires that one measure many contours and/or profiles of that surface, and then average the results. Again, the usual practice is to then add 1 to the average value, so that the fractal dimension ranges between 2 and 3, rather than between 1 and 2.

2.3. Triangle Method

The triangle method is a way of analyzing a a rough (not flat) surface directly, by covering the surface with triangular grids (Figure 8), and using the change in surface area with the change in grid size as the basis of the fractal analysis. The triangles making up the grid are isosceles right triangles, so that two triangles make a square. The elevations of the apices of the triangles are determined by the height of the surface at the apex locations. The area can is found by a standard vector formula given three points (a, b, and c) in x-y-z space, where area

$$A = \frac{1}{2} \text{Abs} \left[(b-a)(c-a) \right]$$

If all three corners are the same elevation, then the triangular surface area is a minimum. The surface is covered repeatedly with a series of different sized grids, and the total area of the triangles is calculated for each grid size. A rough surface will have the elevations different for the three apices and the areas of the triangles will be as large or larger than the minimum value. The total surface area of the rough surface would thus be greater than the total surface area of a flat surface. The total surface area is plotted on the y-axis, and the resolution of (i.e. distance between) the grid points is plotted on the x-axis, on a log-log scale. This is a variation or direct generalization of the divider method, using triangular increments (like rulers) to measure the surface area (instead of the length).

In practice, there is some ambiguity in this technique. Pairs of triangles are positioned over square grid areas (e.g. over a digitized data set). The choice of diagonal can affect the results. One diagonal will be a topographic ridge, while the other will be a topographic valley. The surface area covered by the two sets of triangles with opposite diagonals will not give the same results. Denley (1990) calculates the surface area for both diagonals and uses the average. The results are plotted on a log-log plot as the normalized area versus the grid element size where the surface area is normalized by the frame area (the minimal value possible for surface if it were flat). If the data plot on a straight line, then the surface is defined as a fractal surface. The slope

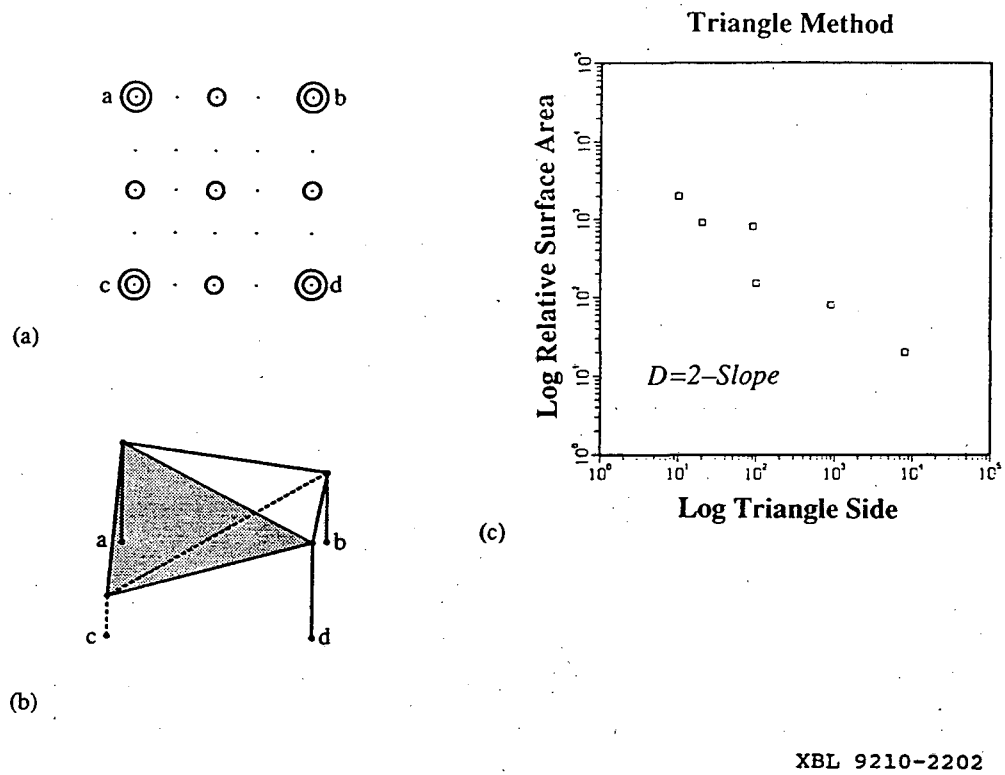

Figure 8. Triangle method: plan view of surface covered with triangles of consecutively smaller size (a); choice of diagonal may give different surface area, solid diagonal gives ridge while dashed diagonal gives valley (b); example of log-log plot where D = 2 - slope; A is area of rough triangle; A_0 is area of flat triangle; Relative surface area is A/A_0. After Denley, 1990.

of the plot (which should be negative) is used to determine D, where D equals 2 minus the slope.

2.4. Slit-Island Method

The slit-island method was first introduced by Mandelbrot et. al. (1984). In this technique, the topographical surface is sliced horizontally, creating a surface contour which divides the surface into two kinds of shapes. One can think of the slice as a water level, where those shapes which emerge above the water are "islands," and those submerged below the water are "lakes." There is a range of sizes of these regions, and the population of different sized islands becomes the basis of the scaling, simplifying the measurement of fractal dimension. Instead of having to measure the islands with a variety of rulers, the islands are measured individually, with both a perimeter and an area value assigned to each island. These parameters are then plotted on a log-log plot of perimeter versus area, and if they plot on a straight line, the slope = 2/D, or D equals 2 divided by the slope (Figure 9). This technique, like the triangle method, is designed to measure a

surface, in contrast to some of the other techniques (e.g. the box and divider methods) which are designed to measure a curve, and must be adapted to measure surfaces.

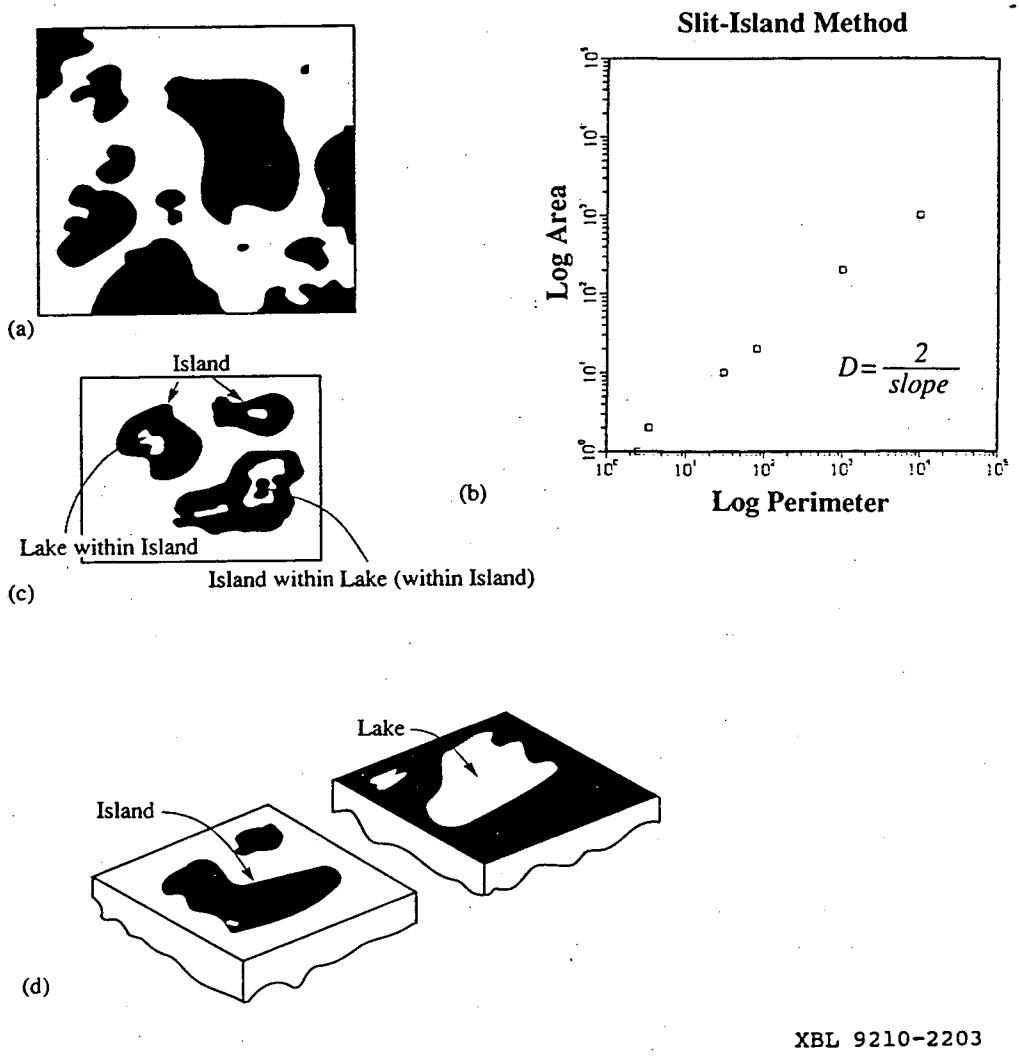

Figure 9. Slit-Island method: take a horizontal cut through the surface creating islands (dark regions) (a); example of log-log plot where D = 2/slope (b); Mandelbrot's "island within lakes" (c); Huang et al.'s "islands within lakes" (d).

One particular problem with this technique is that an island may have within it "lakes within islands" as well as "islands within lakes." This problem was addressed by Mandelbrot et al. (1984) who included "lakes within islands" in the analysis, but neglected the "islands within lakes" (Figure 9). The reason for this choice was probably related to the range of resolution over which the pattern was expected to be fractal. Huang et al. (1990) used both "lakes within islands" and "islands within lakes" in their analysis. However, they were referring to looking at matching sides of the fracture, so that the "lakes within islands" were the complementary shapes on one side of the fracture, and the "islands within lakes" were the shapes on the opposite face of the fracture (Figure 9). They analyzed all of the area versus perimeters of one side of the fracture, then did the same analysis using the other side of the fracture, and these measurements were not the same. For the same surface, it would be interesting to apply the slit-island analyses to the submerged areas instead of to the islands (Figure 9). Is the fractal dimension of the submerged areas ("water or lakes") the same as the fractal dimension of the islands?

2.5. Power Spectral Method

Power spectral methods are based on power spectral analysis, which can be applied to time series data, as well as to vertical profiles taken across topographic surfaces (Berry and Lewis, 1980; Langford et al., 1989; Brown, 1987; Gilbert, 1989). The power spectral density function for random data describes the data in terms of the spectral density of its mean square value for different frequencies (Bendat and Piersol, 1966). Once the data are plotted as power spectral density versus frequency on a log-log plot (Figure 10), the fractal dimension can be determined from the slope of this plot. This technique is favored by geophysicists, and after the divider method, is probably the most popular method of measuring fractal dimension.

This technique requires a considerable amount of pre-processing of the data, described in Power and Tullis (1991) and Bendat and Piersol (1966). The first step is to remove trends from the data. The trends are likely overprinted from spectral components with wavelengths larger than the profile lengths. The linear trend can be determined by least square fitting of a line to the data along a profile. The second step is to taper the profile to handle a remainder problem. This is usually done using a cosine-squared (Hanning) window, so that the beginning and end of each profile begins with a zero. Next, a fast Fourier transform (FFT) algorithm is applied to the data. The FFT algorithm is used to describe the profile data as a sum of sine and cosine waves. The power spectral density can then be calculated by squaring the amplitude at each frequency and normalizing with the profile length. The ensemble averaged spectrum is calculated by averaging power at each discrete Fourier wavelength from multiple profiles of equal length. The spectral density versus the spatial frequency is then plotted on a log-log plot. A straight line is fitted to the plot, and then the fractal dimension is calculated, where $D = (5-\text{slope})/2$. The computed line can be subtracted from the power spectral line to inspect the residuals. If the line fit is acceptable, the residuals should be approximately zero and have no structure (Gilbert, 1989).

The problems with this method are that it requires complicated pre-processing, and these processing techniques vary considerably among different researchers. There are different ways to

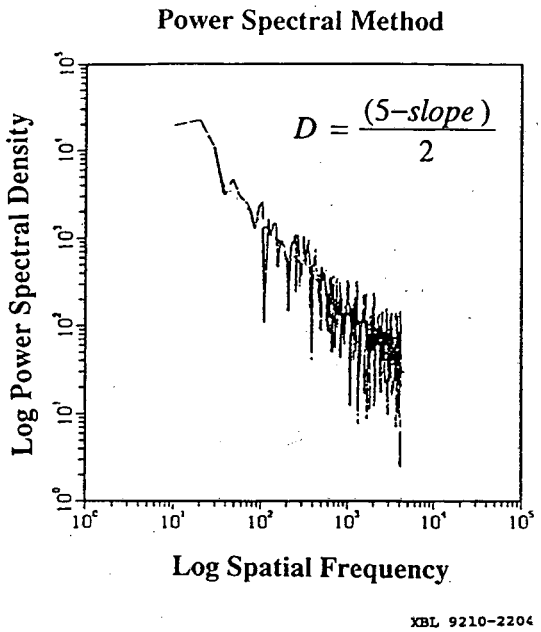

Figure 10. Power spectral method: compute spectral density of profile as a function of frequency and plot on log-log graph; D = (5 - slope)/2.

detrend, to taper, and there are numerous FFT algorithms. Also, the log-log spectral plots are not nearly as linear as are the log-log plots obtained from other techniques for measuring fractal dimension, so that curve-fitting errors can be greater for the spectral method. In addition, the power-spectral method, like the divider and box methods, is designed to measure line patterns, and must be adapted to measure patterns extending over a two-dimensional coordinate system. The common practice is to measure a series of profiles, find an average fractal dimension of the set of profiles, and add 1 to this dimension.

2.6. Variogram Method

The variogram method of measuring fractal dimension relies on a geostatistical analysis of a spatial data set (Burrough, 1983a,b; Wang et al., 1988). The variable could be any property which varies over a plane, including topography, temperature, moisture, and chemical composition. The spatial data set is thus a surface. The spatial distribution of a variable z can be characterized by a variogram of semivariance function. For a profile along an array $z(x_i)$, the semivariance (v) can be estimated as

$$v(h) = \frac{1}{2n} \sum_{i=1}^{i=n} (z(x_i) - z(x_i + h))^2$$

where n is the number of pairs of separated points, separated by a distance h (the lag). When the

estimated semi-variance is plotted against h, it can either asymptotically approach a constant value (sill) or increase without bound as h increases. Unbounded variograms suggest that variation is occurring over a continuous range of scales (Burrough, 1989). Both the transitive variogram with a finite sill and unbounded variograms can be analyzed in log-log plots (Wang et al., 1988). If the log of the estimated semi-variance is plotted against the log of h, the slope is 4–2D. So the fractal dimension can be computed as D = 2–(slope/2) (Figure 11).

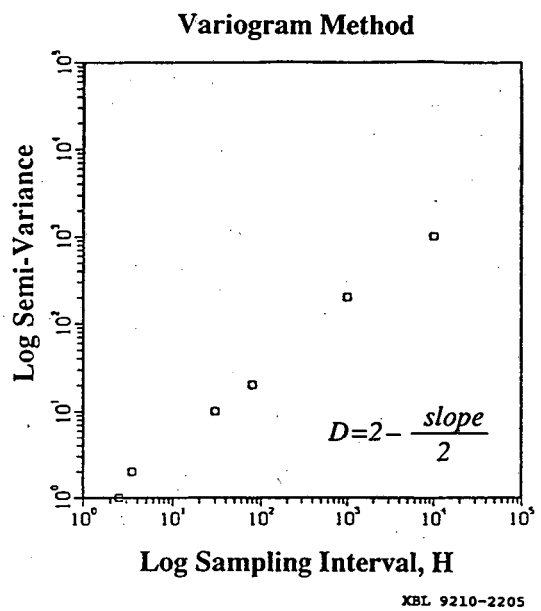

Figure 11. Variogram method: compute semi-variance as a function of sampling interval and plot on log-log graph where D = 2 - (slope/2).

2.7. Distribution Method

Another statistical approach to fractal dimension measurement is to apply fractal theory to a size distribution or histogram (Avnir et al., 1985; Curl, 1986; Krohn, 1988a,b). The sizes (length, area, volume, or any physical or chemical measurement) of a certain phenomenon (mineral grains, caves, etc.) are divided into size classes. The number of objects belonging to each size category are then plotted on a log-log graph, with the number on the y-axis, and the size class on the x-axis (Figure 12). Many size distributions in nature follow Korcak's empirical law (Mandelbrot, 1982) where the probability of an area A exceeding some minimum area a is given by

$$Pr(A > a) = ka^{-B}$$

Mandelbrot (1982) explains that this size distribution is a consequence of fractal fragmentations. If the x-axis parameter is area, and the data fall along a straight line, then the slope of the line

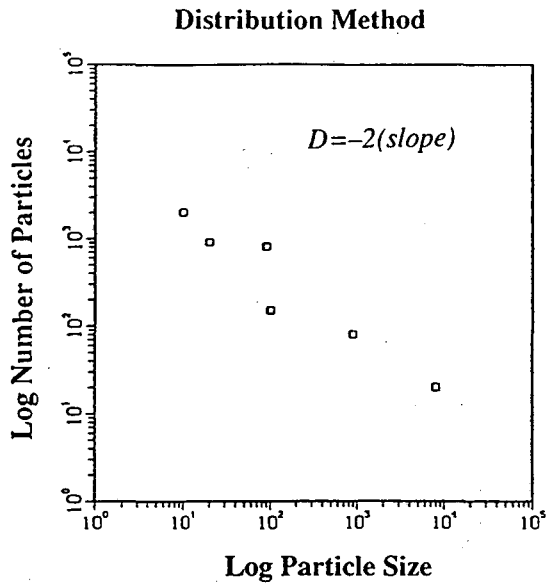

Figure 12. Distribution method: determine the size distribution and plot the log of the size class versus the log of the number of counted objects which are greater than the size class; D= -2 slope, if the size is an area.

equals - D/2 and D = - 2 (slope). Other types of distributions lead to different equations. For example, if a size distribution of particles falls along a line on a log-log graph, (with number of particles exceeding a size class on the y-axis, and diameter on the x-axis), then D = –slope (Rieu and Sposito, 1991b).

3.0. APPLICATIONS IN THE EARTH SCIENCES

Researchers in the earth sciences have applied fractal measurement to numerous types of phenomena over length scales ranging over 15 orders of magnitude, from megameters to nanometers. We have selected examples from the following categories: map data (elevation contours, channels and caves, and fault traces); fracture surfaces (natural rocks and metals); pore geometry (aggregate, particle size distributions); and microscopic surface phenomena (adsorption, dissolution). Map data are used by geographers, geologists, geomorphologists, and geophysicists. Fracture surfaces are studied in the fields of geology, geophysics (rock mechanics), and material science (fractography). Pore geometry is of interest to hydrologists, soil physicists, and petroleum engineers. Surface phenomena are important in the fields of geochemistry, mineralogy, and soil chemistry.

3.1. Map Data (Landscape Scale)

3.1.1. Elevation Contours

Topographic data from the earth are either from land emergent above sea level (mostly continental land masses) or from land submerged below sea level (mostly oceanic floor). Topography of continental land masses is much more heterogeneous than oceanic floor topography, and can be measured by many different techniques. Most ocean floor topography, however, is accessible only by remote geophysical measurement. Following are examples of fractal applications from both types of earth terrain. In addition to earth topography, elevation contours from the surfaces of the other terrestrial planets (Mercury, Venus, and Mars) can be used for studying cratering histories (age relationships) and planetary response to cratering (mechanical response to impact). The fractal theory has been applied to these extraterrestrial types of terrain, but we have not included these examples in this review.

Norton and Sorenson (1989) applied the divider method to topographic map contours of a granitic batholith (a large igneous rock mass intruding older rocks), in the Sawtooth Range in Idaho. They were interested in examining if the fractal dimension could reveal anything about the underlying fracture networks. Fracture patterns of granitic masses reflect the cooling history of the intrusion. Following tectonic uplift of the granites, the exposed fracture patterns are enhanced by surface weathering. Norton and Sorenson digitized contours and vertical sections from maps at scales of 1:250,000 and 1:24,000 and found fractal dimensions ranging from 1.15 to 1.28 within a pluton (small intrusive igneous rock mass). They used a tolerance method to handle the remainder, including only those rulers giving a remainder less than a specified value (tolerance). The data on log-log plots were not linear, but curved concave downwards. They divided the slopes into 3 segments, and used the middle slope to determine the fractal dimension. The fractal dimension correlated most directly with elevation, but also with rock type, fracture abundance and glacial smoothing. Norton and Sorenson concluded that the fractal dimension may have potential use in the analysis of strain and in the correlation of permeability values with fracture networks.

Gilbert (1989) applied the spectral technique to digital elevation data (30 m spacing) from the Sierra Nevada Batholith. The fractal dimension varied between 0.835 and 1.471, depending on the sampling scheme. The lowest fractal dimension was for the entire unprocessed data set. Notice that this dimension is lower than the topologic dimension, so does not fit fractal interpretation; the fractal dimension should be greater than 1 for a line. The spectral density-frequency log-log plots are generally curved with few straight segments. These few straight segments yielded slopes which were a function of bandwidth. Gilbert cautions that if fractal geometry is used to quantify topography, the scale must be specified in the form of the bandwidth being considered, and the data analysis techniques must be clearly stated.

Gilbert (1989) also used the spectral method to determine the fractal dimension of South Atlantic ocean floor topography (425 m spacing). After considerable pre-processing of the raw data, the spectral analysis was applied, and three different processing techniques were compared. The log-log plot of the power spectra versus wavelength was curved, and strongly dependent on

the method of pre-processing. The fractal dimension ranged from 0.919 to 1.325. Notice that the lowest fractal dimension is again less than the topologic dimension, so is inconsistent with a fractal interpretation of the spectra. This indicated that either the profile was not fractal over the band widths considered, or that the data had not been sufficiently processed (Gilbert, 1989).

Matsushita and Ouchi (1989) used a variation of the divider method (see sec. 2.1) to analyze the self-affinity of the topographic data from Mt. Yamigo, Japan. They found that contour lines of topography were self-similar, with a fractal dimension of 1.37. A transect vertical profile was shown to be self-affine with the standard deviations of horizontal and vertical coordinates having different dependence on the curve length. For a transect profile near Mt. Shirouma in the Japanese Alps, the local self-affine fractal dimension for ruler lengths less than 2 km was the same as that for contour lines. The slope of the plot changed at ruler lengths greater than 2 km, giving a larger fractal dimension for global altitude variations.

3.1.2. Channels (caves and streams)

Caves are sub-surface channels created by underground fluid flow. In the case of limestone caves, the fluid is groundwater, while in the case of lava tube caves, the fluid consists of gas and liquids associated with flowing and cooling lava. The caves are geometrically characterized by the lines, areas, and volumes.

Curl (1986) looked at the statistical distributions of cave lengths for ten different geographic locations. The distributions of the number of caves belonging to different size ranges are approximately hyperbolic. By assuming that caves follow a natural fractal distribution, with self-similar property, Curl is able to tackle two problems in cave length measurement: 1) the problem that caves are three-dimensional (volumes) but are measured as lengths and 2) the problem that the measurement length is limited by the size of the person doing the measurement. A person cannot measure a cave if the cave dimension is too small for the person to enter it.

Curl uses a "linked modular element" model where the modulus is a sphere with a diameter of the average explorer. Spheres fill the cave, touching the walls at a minimum of two points. The length of the cave will then be the sum of the sizes of modular elements in that cave, the area will be the total area of modular elements, and the volume will be the total volume of elements. Cave lengths show a fractal dimension of about 1.4, while the fractal dimension of the volume of the Little Brush Creek Cave, Utah, is about 2.8, the same as that of a well-known deterministic fractal called a Menger Sponge.

Streams are surface channels which are much more dynamic than caves, changing course rapidly in response to the changing energy of the stream, which in turn is responding to seasonal changes. Snow (1989) applied fractal analysis to stream channels and related the fractal dimension to sinuosity. Sinuosity is the ratio of real channel length to some general river course length. However, there is no universally applicable objective method of defining river course length. Snow proposes that fractal theory allows one to more precisely define sinuosity. He examined 12 stream channel planforms (map traces of mid-channel stream path) from plateau and lowland regions of Indiana and Kentucky and applied the divider method to them. The mid-channel traces

on topographic maps (1:24,000 scale) were digitized. The log-log plots of trace lengths versus divider lengths from 12 stream channel planforms were compared with each other and with those from idealized meander planforms. Fractal dimensions varied from 1.04 to 1.38. Sinuosity and fractal dimension were related but not directly comparable. Snow found that fractal dimension seemed to be a better way of describing stream wandering than sinuosity.

3.1.3. Fault Traces and Fault Networks

Fault traces are the surface manifestation of the fault planes. These are mapped by geologists and geophysicists, often requiring the synthesis of both air-photo interpretation of topography, and field observations. Large strike-slip fault traces such as the San Andreas Fault have been measured over many different scales. Aviles et al. (1987) applied the divider method to various segments of the San Andreas Fault, focusing on six segments which have some characteristic behavior, such as seismicity patterns, geologic complexity, or historic events. Fault traces were identified on maps, a single predominant strand was selected, and strand ends were joined. This approach involves considerable interpretive processing in the initial selection of the traces. After digitizing the fault traces at every 100 m spacing, data were converted to arc distance, and gaps in data were avoided by joining ends. The traces were very smooth, with fractal dimensions ranging from 1.0008 to 1.0191. However, if one considers the errors involved in selection and measurement, these dimensions are indistinguishable. The short wavelength band showed a larger fractal dimension than the long-wavelength band, and fractal dimensions tended to increase towards the southeast. Fault segments associated with different processes (such as creep, seismic slip, or microearthquake activity) were indistinguishable on the basis of fractal dimension.

In an earlier study of the same data using the spectral method, Scholz and Aviles (1986) found larger fractal dimensions, ranging from 1.1 to 1.5. Okuba and Aki (1987) used the box method on the San Andreas traces, trying to relate strain release to the geometry of the fault traces. They used circles of different radii to cover the faults in such a way as to minimize the number of circles needed to cover a given fault trace. Fractal dimensions fell in the range between 1.12 and 1.43. The fractal dimensions with the box method also increased to the southeast. The fractal dimensions by the box method were somewhat intermediate between those estimated by Aviles et al. (1987) with the divider method and those estimated by Scholz and Aviles (1986) with the spectral method.

In addition to studies of a single fault trace such as the San Andreas fault, the fractal analyses have been applied to a network of fault traces. Hirata (1989) applied the box method to fault systems in Japan, to determine whether or not the structure of the fault system was self-similar. Only those faults which had been active over the past 2 m.y. were analyzed, using geological interpretation of aerial photographs, supplemented by geologic maps and reports. The fractal dimension of fault systems in Japan ranged from 1.05 to 1.60, with high values of 1.5 to 1.6 at the central part of the Japan Arc, and becoming lower outward from the center. There is significant branching in the central part of the arc, and the branching diminishes away from the center. Hirata discussed the relationship between fractal dimension and the energy required to

fracture the rock. The fractal dimension varied with scale, depending on what underlying structure was controlling the fault.

Barton and Larsen (1985) and La Pointe (1988) have measured fractal dimension of fractured networks in rock pavements with areas ranging from 200 to 300 m^2, in an attempt to characterize fracture density and connectivity. Both studies used the box method, placing a size range of grids over the fracture network of three laterally separated rock pavements from a Miocene ash-flow tuff at Yucca Mountain, Nevada. Barton and Larsen counted the fracture intersections for fractures with lengths between 0.20 m and 25 m and found that they fit a log-normal size distribution. The number of grid elements intersected were plotted versus the grid element size on a log-log graph, and the data fit straight lines over the scale range of 0.20 to 25 m, with fractal dimensions between 1.12 and 1.16. La Pointe also placed grids over rock pavements, but used two different formulations to calculate the fractal dimension. In one of these, the number of fractures per unit area of rock is counted for each different grid spacing. In the second formulation, the number of blocks bounded by fractures in each grid cell is counted. La Pointe argues that a block density formulation may correlate better with permeability, because blocks are formed by interconnected fractures rather than by isolated fractures. La Pointe analyzed the fractal dimension of the same Yucca Mountain rock pavements measured previously by Barton and Larsen, using the block formulation and obtained fractal dimensions ranging from 2.37 to 2.69.

3.2. Fracture Surfaces

Fracture surfaces are formed when a solid is stressed beyond its failure threshold and breaks. This involves the disruption of mineral grains, rock fragments, matrix filling, and the breakage of chemical bonds. Natural fractures are then subjected to numerous processes such as movement along the fracture, filling of the fracture by material brought in by fluid flow, and precipitation of minerals in place. Many episodes of these processes complicate the interpretation of fracture surface topography. Laboratory studies, on the other hand, can be controlled so that the fresh surface of rock or metal can be created and measured. Fractal analyses have been applied to both types of fracture studies.

3.2.1. Rock Fractures in the Field and in Hand Specimens

Brown and Scholz (1985) and Power and Tullis (1991) used surface profilers to measure parallel sets of profiles across both laboratory and field-scale rock surfaces. They included different kinds of rock (siltstone and gabbro) and different kinds of surfaces (bedding plane, fractures, glacial scarred surfaces). The spectral method was used to determine fractal dimension of these surfaces. All surfaces showed power spectra which decreased rapidly with spatial frequency. Slopes were determined by least squares fitting of a straight line. Slopes were not constant, and often two breaks in slope were evident, one corresponding to the transition from grain size to larger scale processes, and the other near the outcrop scale (10's of cm). Two of the surfaces were anisotropic, and different fractal dimensions were determined for profiles taken perpendicular to each other. Fractal dimension was constant only over limited ranges of spatial

frequency. Despite these limitations, Brown and Scholz (1985) concluded that the fractal description of fracture surfaces offers an advance over previous topographic measurements because other roughness measures are not constant over any range of scales. The fractal model allows one to tie the topography to natural processes (such as faulting) as well as to numerically develop realistic topographic surfaces (Brown and Scholz, 1985).

Carr (1989) compared the divider and spectral methods for measuring fractal dimension of fracture surfaces in welded tuff from near Yucca Mountain, Nevada. He used two different methods of measuring the surfaces, a stringline method and a photographic technique. The stringline method requires that a string be stretched parallel to a fracture; an elevation is then measured using the string as a base. The photographic technique involves placing a straightedge on exposed rock surfaces to cast a shadow of the surface topography of the rock. This shadow is photographed and a digitized profile is obtained by measuring distance from the straightedge to the top of the shadow. A finer resolution of the rock surface topography was obtained by using the photographic method than by using the stringline method. The profiles obtained from these two measurement techniques were then analyzed by the divider method and the spectral method. The divider method gives a fractal dimension close to 1 while the spectral method yields substantially larger fractal dimensions (Table 3).

Table 3. Comparison of Fractal Measurements

Application	Divider	Box	Slit Island	Power Spectral	Reference
San Andreas Fault Traces	.008-.019	.120-.430	---------	.100-.500	AVILE87,SCHOL85, OKUBO87
Rock Fracture	.410-.500	---------	---------	.510	BROWN87
Joints in Welded Tuff	.000-.020	---------	---------	.500	CARR90
Steel Fracture(vert.section)	.105-.155	.330-.395	---------	---------	HUANG90
Steel Fracture(sec.electron)	.180-.310	.330-.395	---------	---------	HUANG90
Epoxy Fracture	---------	.350	.320	.450	LANGF89
Steel Fracture	---------	---------	.280	.260	MANDE84
Rock Fracture	.058-.261	.041-.159	---------	.124-.383	MILLE90
Titanium Fracture	.099-.126	---------	.320	---------	PANDE87

Miller et al. (1990) measured 60 vertical profiles from rock fracture surfaces of three lithologies (basalt, gneiss and quartzite) and compared four different methods of measuring fractal dimension (the divider, a modified divider, spectral, and box). They found the fractal analysis to be ambiguous and inconsistent, both within a particular method, and between methods. The results of the divider method were found to vary most among the four methods. They tried to find ways to improve the reproducibility of each of the four methods. For the divider method, the results were improved if they divided the remainder by the ruler length, and added this factor to the total length. The modified divider method involves taking equal steps along the baseline,

instead of along the profile. The fractal dimension measured by the modified divider method was generally lower than the fractal dimension obtained by the divider method. Only those rulers which finished within .005 times the length of the baseline were used. For the box method, they obtained best results when the box size allowed 20 to 120 boxes to cover a profile of 1000 digitized points. For the spectral method, the results were most consistent when a 2% to 5% cosine tapering window was used. These guidelines were used in computing and comparing fractal dimensions from the 60 profiles.

They also discussed whether or not the measurement of fractal dimension is consistent with other measurements of roughness. Visual estimates agreed with other methods of quantifying roughness; that is, if one rock fracture looked rougher than another rock fracture, the roughness measurements agreed with the visual assessment. However, the fractal dimension calculated by any of the four methods did not correlate well with the roughness measures, and was often negatively correlated. Therefore, fractal dimension is not necessarily a measure of roughness since it doesn't correlate consistently with other roughness measurements. This conclusion does not exactly contradict that of Brown and Scholz (1987), whose statement was that fractal dimension is a better measure of topography than roughness because of its scale independence. They did not compare or discuss the correlation between roughness and fractal measurement.

3.2.2. Fractures in the Laboratory

Fractures are of interest both for the study of material properties of the solid, and for flow properties of a fluid traveling through the fracture opening or aperture. Fractures in the laboratory have been measured by several techniques. Profilometry was described above for field specimens (Brown and Scholz, 1985; Power and Tullis, 1991). Another technique of measuring fracture aperture is to inject the fracture with a translucent silicone polymer, and to measure the fracture aperture by the attenuation of light passing through the silicone cast of the aperture (Gentier et al., 1989; Cox et al., 1990, 1991). Both profilometry and the silicone cast methods measure the distribution of the thickness of the openings along the plane of the fracture. These spatial distributions of aperture thickness could be used for characterizing flow geometry as well as for determining stress history. The geometry of natural rock fractures has also been studied in the laboratory by injecting molten metal into the fractures in order to determine the geometry and spatial distribution of the contact area of the fracture plane (Pyrak-Nolte et al., 1987; Nolte et al., 1989). Contact area patterns in granitic fractures were measured under different applied pressures by analyzing the filling patterns surrounding the molten metal. The perimeters of the contact areas were analyzed with the divider method, and the fractal dimensions were found to vary from 2.00 to 1.96 as stress on the fracture increased from 6 MPa to 85 Mpa. The distribution of the contact area patterns suggests that critical neck diameters may control the flow, and that the measurement of fractal dimension may help determine flow parameters.

Unlike natural fractures which have been formed by complicated processes in very inhomogeneous materials, the study of fractures in metals and other homogeneous materials offers a way of probing fracturing processes and material properties. The use of fractal analysis to analyze

fractures under controlled laboratory conditions is a very active field of research in materials science, and several examples are presented here.

Mandelbrot et al. (1984) developed the slit-island analysis and presented this technique as a new way of estimating the fractal dimension of fractured metal (steel). The fractal dimension obtained from slit-island analysis was 1.28 while the fractal dimension obtained from the spectral analysis was 1.26. The spectral analysis was based on the average of five vertical profiles. The log-log slopes of the spectral analyses were not smooth, and tended to split into two subregions of different slope. They suggested that these crossover points related to some underlying microstructure. The fractal dimension was shown to depend on the temperature for heat-treated samples, and on the impact energy needed to fracture the metal samples. The fractal dimension increased with temperature and decreased with impact energy.

Underwood and Banerji (1986) generated fractal data from vertical profiles through fractured steel, using the divider method in an automated digitizing program. They found no self-similarity, and the apparent curve length didn't increase without limit as the ruler decreased. Instead of measured length itself, the ratio of the measured length over the projected length was plotted on log-log scale versus ruler length. The plot is not a straight line. However, they used the middle section of the curve to determine a fractal dimension which varied with tempering temperature.

Huang et al. (1990) also studied heat-treated impact fractured steel, using slit-island analyses as well as divider methods applied to vertical profiles. The fractal dimension determined from vertical profiles was very different from that determined from horizontal slices. For both of these methods, the fractal dimension increased with temperature. They found that the results of the slit-island analyses were different for "lakes within islands" versus "islands within lakes," where "lakes within islands" referred to features on one side of a fracture, and "islands within lakes" referred to features on the other side of the fracture. Fractal dimension of "lakes" decreased with increasing impact toughness but the fractal dimension of "islands" increased with increasing impact. This was attributed to the plasticity of the fracturing. They expected that these two fractal dimensions would be the same if the fracturing process was brittle rather than plastic.

Pande and Richards (1987) measured fractal dimension of fractured titanium, using slit-island, divider methods, and secondary electron line-scanning. The secondary electrons are emitted during scanning electron microscopy (SEM) of the surface. The profile of the intensity of the image is then analyzed using the divider method. The slit-island analysis gave a fractal dimension of 1.320. The divider method was applied to two vertical profiles which were polished and observed under the SEM at different magnifications. Fractal dimensions by the divider method ranged from 1.087 to 1.126. The fractal dimension obtained from the secondary scanning electron beams was 1.171.

Langford et. al. (1989) measured fractal dimensions of epoxy fractures. They measured the fractal dimensions of the photons emitted during fracturing as well as the resulting fractured surface. The amplitude and fluctuations of the photons were analyzed both by the spectral method

and the box method. The application of the spectral method to the photon emission profile gave a fractal dimension of 1.45 while the box method gave a fractal dimension of 1.35. The epoxy fracture surface was then analyzed using the slit-island analysis, giving a fractal dimension of 1.32. The correlation between the fracturing process and the fracture surface was attributed to crack branching and void growth. They tried to apply the same analysis to MgO crystals but the relief was too small for slit island analysis, and the spectral analysis did not yield a single slope. Box analysis of photon emission of MgO gave a fractal dimension of 1.16.

Denley (1990) measured fractal dimensions of steel and epoxy fractures, from scanning tunneling microscopy with resolution near 1 angstrom. He used the triangle method to determine surface area of the fractures. Neither material yielded a straight line on a log-log plot of area versus length scale. The log-log plot for steel was convex upwards, while that for epoxy was convex downwards. He estimated a fractal dimension of 2.07 for the steel surface.

Mecholsky and Mackin (1988) measured the fractal dimension of a fractured flint (SiO_2) called the Ocala Chert, used by prehistoric Americans for tool-making. They measured the fractal dimension of fractured flint subjected to different heat treatment. The fractured samples were nickel plated and then encapsulated in epoxy and polished parallel to the fracture plane. Slit-island analysis and divider method were applied to the contours of the islands which emerged with polishing. The untreated flint had a higher fractal dimension (1.32) than the heat-treated flint (1.15 to 1.26), and this was attributed to a change in the microstructure with heating. The strength of the flint directly correlated with fractal dimension, and heat treatment decreased both strength and fractal dimension. Microscopic examination of the untreated and heat-treated flint showed a direct correlation between rough appearance and high fractal dimension.

3.3. Porous Aggregates

Porous aggregates in the earth sciences include volcanic ejecta, sedimentary rocks and unconsolidated sediments, soils, and landfill materials. The texture of porous aggregates is important both for fluid retention and fluid flow through soils and aquifers, particularly in the vadose zone (unsaturated zone above the water table), where air and water compete for available pore space. The existence of micropores on mineral or soil particles creates a micro-roughness along pore channels which may have analogous effects to rough fractures. The spatial variability of soils in the field has also been analyzed with fractal methods.

3.3.1. Pore Geometry

Pore geometry has been imaged and analyzed with fractal theory by Katz and Thompson (1985), Krohn and Thompson (1986), and many others, (see review by Thompson, 1991). Krohn (1988a,b) analyzed the fractal geometry of the pore structure of sedimentary rocks using two techniques. One technique was to use thin sections of the rocks, applying the distribution method to the pore sizes. The other method was to use scanning electron micrographs of the rough rock surfaces, applying an automatic feature counter to determine the statistical distribution of pore sizes at different magnification. Both techniques yielded similar fractal dimensions. Some of the

pore distributions were fractal while others were Euclidean. The pore distribution of novaculite, a very finely crystalline metamorphosed siliceous rock of sedimentary origin, had Euclidean pores. The author suggested that the classification of the pore geometry by fractal dimension could be used to measure the extent of pore alteration by pore filling and cements.

Avnir et al. (1985) analyzed and interpreted, in the framework of fractal theory, previously published data of particle size distributions of aggregates of different origin (carbonates, quartz particles, rock particles, and soil particles). They found distinct fractal dimensions for carbonate rocks of different origin. Etched quartz particles had lower fractal dimensions than unetched quartz particles. The soil particles were shown to have fractal characteristics but the data had interesting and abrupt changes of slope at particle size cutoffs which corresponded to different compositions (such as clays and quartz grains). They also compared shocked and non-shocked rock particles from the Nevada Test Site. The shocked rock had higher fractal dimension (and larger surface area) than the non-shocked rock. Knowing the fractal dimension, the smallest particle diameter could be estimated from the measured surface areas.

3.3.2. Flow and Transport

Schlueter et al. (1991) applied slit-island analysis to pore geometry on scanning electron micrographs from several sandstone cores, plotting the perimeter versus area of pores on a log-log plot. They also looked at SEM images of a single pore in Berea sandstone at different scales of resolution. The perimeter/area ratios of these pore images were then measured and plotted on a log-log plot against scale, and a fractal dimension was calculated. The fractal dimension measured by these two methods, the slit-island and the box method, were compared and were very similar (1.31 versus 1.33, respectively). They next developed a relationship between permeability and fractal dimension, and then used the fractal dimension measured by the slit-island method to predict the permeability of the sandstone. The permeability predicted using the measured fractal dimension was of the same order of magnitude as the permeability measured by experiments.

Empirical relations between water content and hydraulic parameters have been explained using fractal geometry and thin-film physics. Toledo et al. (1990) examined the empirical power law relationship between the hydraulic conductivity (conductivity of the fluid through the pores) and water content, and between matric potential (attraction between water and pores) and water content, where the exponent of water content depends on the fractal dimension of the pore geometry. This relationship could be explained by considering the combination of pressures exerted by thin water films on smooth walls and pendular water occupying smaller irregular pores. Thus, the fractal dimension of the pore-grain interface estimates this thin-film pressure. They applied the empirical relationship to soils for which the hydraulic parameters (conductivity and matric potential) had been carefully measured, and determined the fractal dimension of the pore-grain interface. If the empirical relationships are valid and the fractal dimension can be accurately measured from the pore geometry, then the hydraulic parameters might be estimated from the pore geometry.

Tyler and Wheatcraft (1989) and Rieu and Sposito (1991a,b) use another approach to relate fractal dimension of pore geometry to hydraulic parameters. Tyler and Wheatcraft (1989) estimated the fractal dimension from particle size distributions of soils and then correlated the fractal dimension with a fitting parameter for a soil water retention model. Using the fractal dimension from the particle size distributions of ten soils, they found that the estimated water retention data closely matched the observed data for all but the three coarsest soils. Rieu and Sposito (1991a,b) derived seven predictive equations which used the fractal dimension to relate soil porosity to soil water properties. These equations were based on a fragmented fractal porous medium model, and assumed that pore size and particle size were self-similar, and that the fractal dimension could be determined by the particle size distribution. They tested the equations with available physical soil aggregate data and found good agreement between the predictions and the experimentally determined soil water properties.

Electrical conductivity can be used as a geophysical technique to study porosity, permeability, and fluid saturation. Ruffet et al. (1991) measured the electrical responses as a function of frequency for numerous rock samples of varied lithology (sandstones, slate, shale and granites). They used two fractal models to derive the fractal dimension of the samples. One of these models describes a linear transfer process through a fractal interface, and was derived for one-dimensional and modified for two-dimensional fractal media. The other model considers pore surfaces as self-affine fractals, where the rock behaves like a system with resistance in parallel, with particles diffusing along the interface. By plotting the fractal dimension versus the specific surface area for the two models, they determined that the modified 1-dimensional model based on a transfer process was more appropriate, because the fractal dimension increased with surface area, while the other model showed an inverse relationship between fractal dimension and surface area.

3.3.3. Spatial Variability

Mechanical properties of soils, such as compaction and soil strength, are important for the behavior of surface water, for the growth of plants, and for the stability of structures such as buildings and roads. Armstrong (1986) looked at soil surface strength measured with field cone penetrometers and shear vanes, as well as microtopography measured with a profile meter. He used the variogram method, with measurements made between distances of 1 to 1000 meters, over a permanent grassland and a ploughed field in England. The variograms for strength from the grassland soil had very well-defined fractal dimensions between 1.90 and 1.95, while those from the farmed soil were more variable, with values between 1.76 and 1.97. The topographic data for the profiles have fractal dimensions which varied with the number of points used to estimate the slope, and depend on whether or not trend is removed. Armstrong states that many of the practical problems are associated with a lack of a firm theoretical basis for the derivation of the fractal dimension from the variogram.

Burrough (1983 a,b) applied the variogram technique to many different published and unpublished data sets from soil properties measured in the field. These properties included pH,

sodium content, stone content, thickness of soil horizons, electrical resistivity, chroma, bulk density, groundwater level, and particle size fraction. He found that soil properties (obtained from soil auger samples) such as percent clay, percent silt, or pH, were fractal but not self-similar. He found that soils data usually have a higher proportion of short-range variation than landform or groundwater surfaces, which is reflected in high D values (greater than 1.5). He proposed the use of a nested model of one-dimensional soil variation, where identified soil processes occurring over identifiable scales can be used deterministically, to make prediction or interpolation. However, the nested model was not appropriate when the variation occurred at many closely related scales, with the superposition of these processes. That is, the nested model worked best where lateral mixing was negligible and soil boundaries were sharp.

3.4. Microscopic Surface Phenomena

The application of fractal analysis to microscopic surface phenomena is a very active area of research, and includes such phenomena as surface adsorption, aggregation of particles, and mineral dissolution. The fractal theory has been applied to static geometry, such as surfaces of minerals (clay), and to dynamic processes, such as the growth of particle aggregations and the erosion of minerals.

The fractal dimension of microscopic solid surfaces may be of two different types, surface fractal dimension or mass fractal dimension (Pfeifer and Obert, 1989; Figure 14). Microscopic phenomena are often studied using scattering methods (such as small-angle x-ray, neutron, and visible light scattering) where a fraction of the source beam is scattered when it strikes the sample at different scattering angle. The structure of the sample affects both the intensity of the scattered beam and the scattering angle. Depending on wavelength and scattering angle, these techniques can be used to determine the fractal structures either of the surfaces, with dimensions between 2 and 3, or of the mass distribution, with dimensions between 1 and 3 (Schmidt, 1989; Martin and Hurd, 1987).

Surfaces usually exhibit fractal characteristics on length scales appreciably smaller than the diameters of the mass fractal aggregates. For a mass fractal of aggregates, it is usually assumed that individual aggregate units are identical, rigid (hard), and spherical scatterers. The scattered intensity depends on the structure factor which is calculated by averaging the pair-correlation function over all orientations and over all scatterers in the aggregate. For a surface fractal, the entire sample can be considered to be a single scatterer. The scattered intensity depends on the shape or form factor of the scatterer. In log-log plots of scattering intensity I versus momentum transfer q, one can determine whether a sample is a mass or a surface fractal by the magnitude of the slope, where $I \approx q^{D_m}$ for mass fractals, $D \leq 3$; and $I \approx q^{6-D_s}$ for surface fractals, $3 < 6-D_s \leq 4$).

Figure 14 illustrates the difference between mass and surface fractals (Pfeifer and Obert, 1989). Surface fractal dimension is concerned only with a boundary, either a profile or a contour. The surface fractal defines an area relative to the boundary, and the area is proportional to the measuring radius raised to the power of the surface fractal dimension. Mass fractals depend on the entire solid, and not just the boundary. The system of a mass fractal is described with a lattice

representation; the sites are then either mass sites (occupied sites), surface sites (occupied sites adjacent to unoccupied sites), or pore sites (empty sites). The number of sites occupied by each of the 3 types of sites is counted within a radius R of the site, and the mass is then proportional to the radius raised power of the mass fractal dimension. For a mass fractal the mass sites and the surface sites have the same fractal scaling.

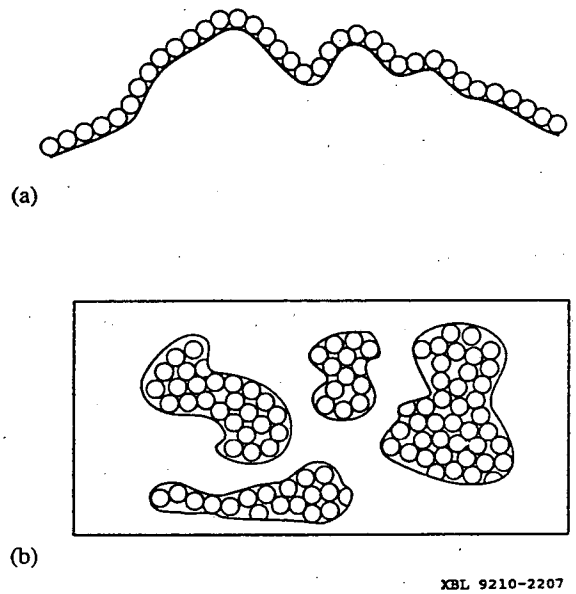

Figure 13. Surface (a) and mass (b) fractal measurement.

3.4.1. Surface Adsorption

Chemically active surfaces are traditionally regarded as two-dimensional flat arrays of atoms or molecules. If the actual surfaces diverge from the flat planar idealization, then estimates of surface area will not be realistic. This problem can be approached with fractal analysis (Pfeifer and Avnir, 1983). The fractal dimension of very small particles can be determined indirectly by measuring the surface area of particles of known diameter and plotting the log of the surface area versus the log of the diameter. This approach was taken by Avnir et al. (1985) who used particles of known radii to study the change of apparent monolayer values with the change in the average radius of spheroidal particles. Powdered samples of various minerals (carbonates, quartz, oxides, etc.) were sieved into several fractions, and for each fraction, the apparent monolayer value was determined by adsorption of some probe molecule such as nitrogen. If the slope of particle size versus radius (or area versus radius) is linear on a log-log plot, then the fractal dimension is obtained from the slope.

Pfeifer et al. (1989) compared two theories (Brunauer-Emmett-Teller or BET and the Frenkel-Halsey-Hill or FHH theories) for multilayer adsorption of gases onto fractal surfaces. At high coverage of the surface by the adsorbate, surface-adsorbate interactions were very different depending on whether the solid substrate was a mass or surface fractal. Fractal BET and FHH isotherms applied to mass and surface fractals, respectively. The BET model with short-range surface-absorbate potential is applicable for mass and surface fractals at low coverage while the FHH model with long range potential is for multi-layer adsorption.

Thermodynamic equations for physical adsorption of gases and vapors on fractal surfaces of heterogeneous microporous solids were derived by Jaroniec et al. (1990). They analyzed various thermodynamic quantities (the differential molar enthalpy, the immersion enthalpy, the differential molar entropy, and the average adsorption potential). All of these quantities increased as the fractal dimension increased. They interpreted this relationship as the gradual filling of micropores. The proportion of narrow micropores increases with increasing fractal dimension of the surface.

3.4.2. Particle Aggregation

Particle aggregation is the nonequilibrium process that governs how particles aggregate to form larger and more complex structures. Examples of particle aggregation include the growth of gold or silver crystals from colloidal suspensions, the growth of bacterial colonies, the aggregation of atmospheric smoke, and the aggregation of stellar material into nebulae. Growth by particle aggregation can provide a model for diverse phenomena including physical aggregation, chemical aggregation, and biological growth. The Witten-Sander type of fractal clusters are simulated or grown by diffusion-limited aggregation (DLA). We mention this topic because it is an active area of very intense research using fractal simulations to explain aggregation and growth processes. It is, however, outside the focus of this review on fractal surfaces. Many excellent reviews of this topic have been published, including Sander (1985), Jullien and Botet (1987), Avnir (1989), and Meakin (1991).

3.4.3. Erosion and Chemical Dissolution

Mineral dissolution is important for the study of weathering processes, and is of interest to geologists and soils scientists. One example from the medical literature illustrates the applications of fractals to the study of organic mineral erosion. In this application Akbarieh and Tawashi (1989) studied the dissolution of Ca-oxalate dihydrate crystals in urine at different pH and solution concentrations, and applied fractal analysis to the surface contours of the crystals. They found that the fractal dimensions for the shape parameters were significantly different for normal urine versus stone-forming urine, and used fractal dimension for medical screening of patients with potential for kidney stone problems. A light microscope was connected to an image analyzer and the perimeter was measured at different scales and length versus scale was plotted on a log-log graph. They also looked at dissolution rate as a function of pH, and this allowed them to see that the mass transfer or erosion from the surface was controlled by both the phase transition of

Ca-oxalate diphosphate to Ca-oxalate monophosphate and by diffusion. Both ionic and non-ionic inhibitors played a role in the process.

Erosion and dissolution may also be studied as dynamic growth processes, where fractal fingering patterns can be explained by diffusion models similar to the particle aggregation growth models. This has applications for the interpretation of fossilized patterns on shales, as shown in Van Damme (1989). There are many fossilized patterns which appear to be biological (dendrites) but which have been formed by viscous fingering. A better understanding of the processes which form these fractal fingering patterns could lead to a better understanding of Earth's early history.

4.0. DISCUSSION OF MEASUREMENT METHODS

We identified and described seven techniques to measure fractal dimension of surfaces. We found that natural surfaces do not have a unique fractal dimension; the fractal dimension seems to be very dependent on measurement method, and may differ even within a single measurement technique. Yet, the application of fractal geometry to problems in the earth sciences ultimately depends on the accuracy and reproducibility of fractal measurement, at least within a single method, if not between different methods. Several of the studies we reviewed compared two or more of the seven techniques for measuring fractal dimension. These are listed on Table 3. From this small grouping, it appears that there may be a tendency for some methods to measure systematically higher fractal dimensions relative to other methods.

Four of the methods for measuring fractal dimensions of surfaces require taking either vertical profiles (divider method and spectral method) or horizontal cuts (box method, slit island method). Only the triangle method combines the horizontal and vertical slices into one measurement. The theory of fractals implies that an isotropic, self-similar fractal surface should have the same fractal dimension, whether one measures the dimension from vertical profiles or from horizontal contours. However, if a surface is self-affine rather than self-similar, with vertical properties changing at a different rate with scale than horizontal properties, then vertical profiles and horizontal slices would measure different fractal dimensions. Thus, it is not surprising that the same surface would have different fractal dimensions, depending on whether one measured it with vertical profiles or horizontal contours.

Most of the fractal dimensions measured by the divider method were lower than those measuring the same surface by other methods, including other methods using the same orientation. As discussed in section 2.1 above, the divider method often gives fractal dimensions near one. One explanation for this low fractal dimension is that when a surface scales differ in the horizontal and vertical directions, and the horizontal resolution is near the crossover length, the fractal dimensional increment will be near zero (Brown, 1987). Brown suggests magnifying the profile height repeatedly until a stable fractal dimension is obtained. Most of the divider method measurements presented in Table 3 did not address this problem, and this may explain why the fractal dimensions found with the divider method are so low.

Most fractal dimensions measured by the power spectral method were larger than those measuring the same surface by other methods. Aside from the problems of measurement

resolution near the crossover point, there may be other more fundamental differences between the spectral method and the other techniques. The spectral method uses integral transformations, while the divider method approximates segments of curves with straight lines, and one might speculate that the difference between integral measure and differential measure may contribute to differences between these two methods.

Fox (1989) applied the divider method to a discrete random series of specified spectral forms in order to compare the divider and power spectral methods. He found that the power spectral relationship for computing the fractal dimension did not hold over the entire range of analysis, and that the relationship between fractal dimension and power spectral exponent was not linear over all fractal dimensions. He found that the spectral technique tends to overestimate the fractal dimension at lower values of D, and to underestimate the fractal dimension at higher D values. Also, Fox found that fractal analysis could not distinguish stationary and non-stationary surfaces. Here, stationary means that the mean value of all profiles taken through the surface should be identical, while a non-stationary surface would have trends. Yet both the divider and power spectral techniques assume homogeneity over the measured interval. The power spectral method requires pre-processing to remove trends; the divider method, as currently applied, does not require any trend removal. He suggests the need for some statistical foundation for using the divider method.

The fractal dimensions measured by the box and slit-island methods listed on Table 3 are high if compared to divider method, and low if compared to spectral method. There was only one study which compared box and slit-island methods and this showed a slightly lower D value for slit-island. The box method and slit-island method are comparable, because both methods analyze horizontal cuts. The basic difference is that the slit-island method assumes that the size distribution of the population of shapes reflects the self-similarity, while the box method requires the measurement of all of the shapes at different scales. It is possible that interactions between processes and materials may be such that the population of large shapes may be different from the population of small shapes. Large features, for example, might be formed of different material from smaller features, and this would lead to a non-linear slope on the log-log graph for the slit-island analysis. However, the box method applied to the same data would consider all of the shapes at every scale, so that an average would be derived from the data, and this might result in a straight line, and a different fractal dimension.

Only a sample of the surface can be used for measuring fractal dimension, and there are no rules as to what is a proper sample. A set of north-south vertical profiles may give a different fractal dimension than a set of east-west or radial vertical profiles. What about horizontal cuts? Should a set of contours at different cutoffs be used as the sample, or a single contour or cutoff? What happens if the slice is not vertical or horizontal but inclined? If the fractal dimension changes between different profiles, or between different horizontal cuts, what type of averaging (arithmetic, harmonic, geometric) should be used to determine the fractal dimension of the whole surface? Or does the absence of stationarity and self-similarity indicate a situation where fractal analysis should not be applied?

There are several operational problems common to all of the direct measurement techniques. One of these is the problem of the remainder. For the divider method, as one approaches the end of the curve, there will be some quantity which won't fill the last ruler. Aviles et al. (1987) discuss three ways of handling the remainder. One way is to use only those rulers which give a remainder less than a specified value or tolerance. A second way is to add the straight-line distance between the ruler and the end of the curve to the total length. A third way is to round up the remainder. The choice of method for handling the remainder may lead to different estimates of fractal dimension, and these differences should be considered as part of the error of the measurement. If the approach of marking segments along a baseline is used instead of marking segments on the curve, then the remainder problem can be avoided, by recursively subdividing the total length of the baseline into halves. There is also a potential remainder problem with the box and triangle methods. As the grid coarsens, there may be some area which doesn't fit the new discretization. The spectral method handles the remainder problem by normalizing the power spectral density with the profile length, and by tapering. The slit-island method also has a remainder problem, which hasn't been addressed in the literature. What happens to islands which cross the boundaries of the field of study (Figure 9a)? Should they be ignored, or partially counted?

Another operational problem of fractal dimension measurement is the estimation of the slope from the log-log plot. There is no consistent way of estimating the slope, and different methods can give considerably different results. The slope may be estimated by a linear regression, or other standard curve-fitting techniques. Often, only part of the plot will be used to calculate the slope, while other researchers will use the entire plot. The slope is often somewhat curved, rather than straight. Does this curvature indicate that the fractal theory is not applicable to that particular data set, or is this just the expression of lack of self-similarity of the data? What does it mean if the curve is concave up versus concave down? Some researchers choose a particular straight section of the curve for the estimation of slope, explaining that the straight segment is the range of scales over which the fractal theory applies. If an error analysis were applied to the slope estimation, the error range for the fractal dimension could be as large as the possible range of fractal dimensions. Many of the studies do not estimate errors, or they estimate only one aspect of the error, such as the curve-fitting error, while ignoring others such as the remainder error.

Fractal dimension measurement would benefit from having some means of calibration, so that the measurement method could be applied to some standard profiles or surfaces with known fractal dimensions, and a correction factor applied if necessary. Aviles et al. (1987) calibrated the divider method by applying it to the west coast of Britain which Mandelbrot had previously measured ($D = 1.25$; Mandelbrot, 1982), and to von Koch curves ($D = 1.262$). If a measurement method is calibrated on map data and compared with another researcher's measurement of fractal dimension of that data, then both the range of scales and the map must be the same for the previous measurement and the new measurement.

Another consideration which is somewhat related to calibration is that of the range of acceptable fractal dimensions for the data set under consideration. What if fractal dimension is less than Euclidean dimension? Several of the studies reviewed in this paper showed a fractal dimension which was less than the Euclidean dimension of the surface. Does this mean that the surface is not fractal? On the other hand, what if the fractal dimension is greater than 2.5? Operationally, it may not be possible to measure a surface which has a fractal dimension greater than 2.5. If the fractal dimension of a physical surface is greater than 2.5, then the surface begins to curl, creating overhangs and tunneling depressions. If this were a solid phenomenon, such as a sandstone which has partially dissolved cement at the surface, then a horizontal profile through the sandstone would curl under around the rounded grains (Figure 14). A landscape-scale example of this problem is that of overhanging cliffs and of caves. If this type of surface is not measurable, how does the presence of overhangs distort the accuracy of the fractal dimension measurement? If there are no overhangs or caves, is it possible to have a fractal dimension (of a surface) exceeding 2.5?

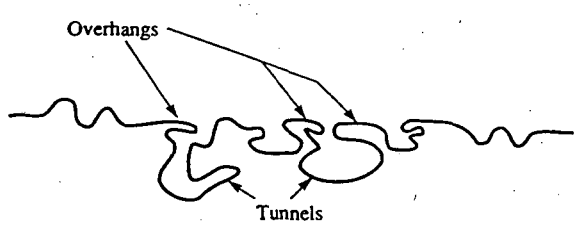

XBL 9210-2208

Figure 14. Overhangs: this profile has both overhangs and tunnels, both of which may present measurement problems.

The fractal dimensional increments shown in Table 1 indicate that the variogram and distribution techniques, in general, measure much higher fractal dimensions than the more direct methods. Burrough (1983; 1989) applied the variogram method to soils data, and explained that the high fractal dimensions indicated the high local variability of soils properties. Sandstone pores measured by the distribution method also showed fractal dimensional increments greater than 0.5. The sandstone pores and cave distributions are volume fractals, rather than surface fractals. Measurements of volume fractal dimensions seem to have increments above 0.5, while those of surface fractal dimensions seem to have increments below 0.5. Does the fractal dimensional increment change as Euclidean dimension changes? Most of the papers we reviewed implied that the increment doesn't change with Euclidean dimension, so that one can take the fractal dimension of a line (such as a profile or a contour) and simply add 1 to make it a surface, or 2 to make it a volume. Yet Curl's (1986) analysis of cave distributions showed that the fractal dimensional increment was not the same for different lines versus volumes (Table 3). The fractal dimension of cave lengths was around 1.4, while fractal dimension of cave volume was 2.8, not 2.4. Similar studies to probe the potential inconsistency among profile, contour, surface, and volume measurements are needed.

5.0. DISCUSSION OF APPLICATIONS

Most of the applications reviewed in this report have been listed on Table 1, along with the method used, and the fractal dimensional increments obtained. Applications of fractal measurement to problems in the earth sciences seem to fall into a few general categories. These include testing whether or not some feature is fractal; characterization of surface geometry to determine some internal property; use of fractal geometry to study formation and degradation processes; use of fractal slopes to determine multiple processes and the scales over which they are dominant; use of fractal geometry as a tool for interpolation and extrapolation; and use of fractal geometry to derive empirical equations to estimate parameters which are difficult to measure.

The first group of studies aims to determine if some feature being measured is self-similar or self-affine (Hirata, 1989; Matsushita and Ouchi, 1989) or to evaluate the reproducibility and accuracy of of fractal measurement techniques (Gilbert, 1989; Carr, 1989; Miller et al., 1990). The primary criteria for determining the self-similarity of a surface is based on whether or not a straight line can be fitted to the log-log plot of the measurement versus resolution. If the slope of the line depends on the orientation of the sampling, then the surface is considered to be self-affine instead of self-similar, and the data can then be transformed, in principle, by rescaling to determine the fractal dimension for the data set. The log-log plots in many earth science studies in this review appear to be very scattered and do not follow the idealized model with a simple straight line. When the log-log plot is not linear and no unique slope can be determined, there is a need for procedures to systematically go beyond simple fractal analysis and extract useful information or parameters from the nonlinearity of the log-log curves. If we use a statistical approach, fractal dimension is likely to be a lowest order parameter, to be complemented by a class of higher order parameters to characterize the scaling properties of spatially distributed data.

Several studies used fractal measurement to characterize some surface in order to determine its underlying structure or some internal property. This category includes the measurement of topography by Norton and Sorenson (1989), who found some correlation between fractal dimension and elevation, rock type, fracture abundance and glacial smoothing. Barton and Larson (1985) and La Pointe (1988) characterized fracture networks in order to correlate these characterizations with fracture density and connectivity. The laboratory studies of fractal geometry of rock fractures also fit under this category (Pyrak-Nolte et al., 1987; Nolte et al., 1989; Mandelbrot et al, 1984; Underwood and Banerji, 1986; Huang et al., 1990; Denley, 1990; Mecholsky and Mackin, 1988), where the fractal dimension of fracture features is measured under different physical conditions, to see if there is any relationship between the underlying physical structure and the measured fractal dimension. One problem with this application is that the surface fractal is being used to determine an internal structure which is a property of the entire rock mass. The change in the physical structure in the three-dimensional coordinate system may not be accurately represented by a measurement of the surface fractal dimension.

A third general category for applications is the measurement of fractal geometry in order to determine something about formational or degradational processes. Akbarieh and Tawashi (1989) studied dissolution of crystals in urine as a function of fractal geometry in an attempt to

screen patients at risk for kidney stones. Van Damme (1989) suggested the use of fractal measurement to aid interpretation of fossil patterns. Langford et al. (1989) tried to relate the fracturing process to crack branching and growth through the fractal dimension. Pore geometry studies such as that of Krohn (1988 a,b) tried to relate fractal geometry to the extent of pore alteration by pore filling and cements. To what degree does the fractal analysis improve or enhance more conventional analyses? This will need to be determined separately in different applications.

A fourth general category is the use of fractal geometry to unravel multiple processes, and to determine the scales over which these processes are dominant. The studies of the San Andreas Fault trace (Okuba and Aki, 1987; Aviles et al., 1987; Scholz and Aviles, 1986) and the measurement of field and laboratory fractures (Brown and Scholz, 1985; Power and Tullis, 1991) were focussed on determining the ranges of spatial scales over which the fractal dimension was invariant. Burrough (1983 a,b) looked at nested variations of soil properties. One challenge for these types of applications is to separate the inflection points which separate log-log slopes which differ due to anisotropy (self-affine fractals) from those inflection points which separate slopes which differ due to multiple processes with different scaling properties. One approach to fractals which display multiple scaling is multifractal analysis (Lovejoy and Schertzer, 1991).

A fifth category for fractal applications is the use of fractal measurement for interpolation and extrapolation. Curl's (1986) use of cave length distributions to extrapolate volumes and lengths of small caves is an example of this category. Snow's (1987) use of fractal measurement of streams, as a measure of stream length or wandering, is another example. Burrough (1983a,b) tried to relate fractal distributions to the interpolation of data measurements over a large field. These types of applications may enable the refinement of conventional statistics and geostatistics.

Finally, the last general category is the use of fractal measurement to derive some empirical equation in order to estimate some other parameter which is difficult to measure experimentally. Tyler and Wheatcraft (1989) derived equations for soil water retention as a function of fractal dimension. Schlueter et al. (1991) tried to relate fractal dimension of pore geometry to permeability. Toledo et al. (1990) related hydraulic parameters to fractal geometry using thin-film physics. Rieu and Sposito (1991a,b) derived several relationships for soil physics from distributions using the fractal dimension as the measurable parameter. Pfeifer et al. (1989) and Jaroniec et al. (1990) tried to use correlations between fractal dimension and physical chemical properties in order to refine surface adsorption theories. This category of application is very specific to the particular study, and may depend on new conventions of recording experimental data.

6.0. CONCLUSIONS

Based on the literature review performed in this report, we reach the following conclusions.

(1) Fractal dimension may vary systematically with measurement method.

The measurements listed in Tables 1 and 3 show several tendencies. Divider methods tend to give low values for fractal dimension. The reasons for this may have to do with the self-affinity of the natural surfaces. Corrections suggested by Brown (1987) and by Matsushita and Ouchi (1989) should be further evaluated. Power

spectral methods tend to give high values for fractal dimension. Also, power spectral methods require many processing steps, introducing potential variations due to different methodology at each step. Power spectral log-log plots tend to be much more curved than the other log-log plots. This introduces more uncertainty in curve-fitting. Box methods and slit-island methods tend to give fractal dimensions in the intermediate range. We have found only one publication which utilized the triangle method. Since this technique simultaneously measures the horizontal and vertical variation, both the self-affinity and self-similarity are involved. A statistical analysis of measurements made by all of the different methods over a set of surfaces could help verify the tendencies shown in Tables 1 and 3. Fox (1989) did this for the power spectral and divider methods and concluded that there were non-linear systematic differences between these two methods.

(2) Operational steps in the measurement of fractal dimension and the underlying assumptions of each measurement step need to be scrutinized.

The operational steps include orientation of data, size and direction of sampling, remainders, slope estimation, error of measurement, and interval over which fractal dimension is measurable. Problems concerning orientation of the measurement plane, as well as considerations of what constitutes a valid sample for fractal dimension measurement need to be clarified. Remainder problems and boundary problems need to be considered and clearly stated when applying fractal measurement to research problems. Except for the triangle method, the other four "direct methods" require the transformation of a line to a surface. The assumptions made for this transformation to be valid need to be better understood. There needs to be a better conceptual understanding of what the measurable ranges of fractal dimension imply, as well as an understanding and statement of the cumulative error involved in measurement. There is a need to better understand the shapes of the curves, what that shape implies, and when, where, or how it is valid to convert that data to a straight line. The present means of "calibrating" fractal dimension, i.e., by using deterministic fractals such as von Koch curves, or by using the coastline of Britain, need to be evaluated. Are there better ways of calibration? The concepts of fractal population distributions are different from fractal analysis of a boundary. The assumptions made when one uses the slit-island technique (a population distribution) to measure a boundary (such as a fracture surface) need to be clarified.

(3) Fractal models need to be used with caution in earth sciences applications.

We reviewed various applications of fractal models in the earth sciences. Applications tend to fall in 6 categories: measurement to determine the validity of fractal theory or measurement techniques; characterization to determine underlying structure; using fractal geometry to determine formation or degradation processes; analyzing fractal slopes to determine multiple processes and the scales over which a process is dominant; interpolation and extrapolation; and the derivation of empirical equations based on measured fractal dimension in order to determine some hard-to-

measure parameter. The fractal dimension may allow the extraction of information embedded in the data which would not otherwise be visible. However, the usefulness of fractal measurements in the earth sciences has not yet been clearly demonstrated.

7.0. ACKNOWLEDGEMENT

The authors gratefully acknowledge critical review by Drs. Robert Zimmerman, Steve Martel, Nigel Quinn, and Yvonne Tsang, all of the Earth Sciences Division, Lawrence Berkeley Laboratory. Valuable discussion and suggestions were given by Professor Garrison Sposito, University of California, Berkeley. This work was supported by Sandia National Laboratories, and the Director, Office of Civilian Radioactive Waste Management, Yucca Mountain Site Characterization Office, Regulatory and Site Evaluation Division under U. S. Department of Energy Contract No. DE-AC03-76SF00098.

8.0. REFERENCES

Akbarieh, M. and Tawashi, R., 1989. Surface studies of calcium oxalate dihydrate single crystals during dissolution in the presence of stone-formers' urine. Scanning Microscopy 3(1): 139-146.

Armstrong, A. C., 1986. On the fractal dimensions of some transient soil properties. J. Soil Science 37:641-652.

Aviles, C. A., Scholz, C. H. and Boatwright, J., 1987. Fractal analysis applied to characteristic segments of the San Andreas Fault. J. Geophys. Res. 92(B1):331-344.

Avnir, D.(ed.), 1989. The Fractal Approach to Heterogeneous Chemistry: Surfaces, Colloids, Polymers. John Wiley and Sons, 441 p.

Avnir, D., Farin, D. and Pfeifer, P., 1985. Surface geometric irregularity of particulate materials: the fractal approach. J. Colloid and Interface Science 103(1):112-123.

Barton, C. C. and Larsen, E., 1985. Fractal geometry of two-dimensional fracture networks at Yucca Mountain, southwestern Nevada. Proc. Internat. Symp. Fundamentals Rock Joints, 15-20 September, 1985: 77-84.

Bendat, J. S. and Piersol, A. G., 1966. *Measurement and Analysis of Random Data.* John Wiley & Sons, New York, 390 p.

Berry, M.V. and Lewis, Z. V., 1980. On the Weierstrass-Mandelbrot fractal function. Proc. R. Soc. Lond. A 370: 459-484.

Brown, S.R., 1987. A note on the description of surface roughness using fractal dimension. Geophys. Research Lett. 14 (11): 1095-1098.

Brown, S. R. and Scholz, C. H., 1985. Broad bandwidth study of the topography of natural rock surfaces. J. Geophys. Research 90(B14):12,575-12,582.

Burrough, P. A., 1983a. Multiscale sources of spatial variation in soil. I. The application of fractal concepts to nested levels of soil variation. J. Soil Science 34:577-597.

Burrough, P. A., 1983b. Multiscale sources of spatial variation in soil. II. A non-Brownian fractal model and its application in soil survey, J. Soil Science 34:599-620.

Burrough, P. A., 1989. Fractals and Geochemistry, in "The Fractal Approach to Heterogeneous Chemistry" (D. Avnir, ed.). John Wiley and Sons, pp. 383-404.

Carr, J. R., 1989. Fractal Characterization and Joint Surface Roughness in Welded Tuff at Yucca Mountain, Nevada. Proc. 30th U.S. Symp. Rock Mechanics, Morgantown, West Virginia, (A. W. Khair, ed.), Balkema, Rotterdam, pp. 193-200.

Cox, B. L., Pruess, K., and Persoff, P., 1990. A casting and imaging technique for determining void geometry and relative permeability behavior of a single fracture specimen. Proc. 15th Workshop Geother. Reserv. Eng., Stanford Univ., 6 p.

Cox, B. L., Pruess, K., and Persoff, P., 1991. Evaluation of a casting-and-imaging technique for measuring void geometry of fractured rock specimens, Earth Sciences Division Annual Report 1990, (LBL-29700), pp. 12-15.

Clark, N. N., 1986. Three techniques for implementing digital fractal analysis of particle shape. Powder Tech. 46: 45-52.

Curl, R. L., 1986. Fractal dimensions and geometries of caves. Mathemat. Geol. 18 (8):765-783.

Denley, D. R., 1990. Practical applications of scanning tunneling microscopy. Ultramicrosp. 33:83-92.

Falconer, K., 1990. Fractal Geometry: Mathematical Foundations and Applications. John Wiley and Sons.

Fox, C. G., 1989. Empirically derived relationships between fractal dimension and power law form frequency spectra. Pure and Applied Geophys. 131 (1/2): 211-239.

Gentier, S., Billaux, D., and van Vliet, L., 1989. Laboratory testing of the voids of a fracture. Rock Mech. Rock Eng. 22: 149-157.

Gilbert, L. E., 1989. Are topographic data sets fractal? Pure and Applied Geophys. 131 (1/2): 241-254.

Hirata, T., 1989. Fractal dimension of fault systems in Japan: fractal structure in rock fracture geometry at various scales. Pure and Applied Geophys. 131 (1/2):157-170.

Huang, Z. H., Tian, J. F., and Wang, Z. G., 1990. A study of the slit island analysis as a method for measuring fractal dimension of fractured surface. Scripta Metallur. et Material. 24:967-972.

Jaroniec, M., Lu, X., Madey, R., and Avnir, D., 1990. Thermodynamics of gas adsorption on fractal surfaces of heterogeneous microporous solids. J. Chem. Phys. 92 (12):7589-7595.

Jullien, R. and Botet, R., 1987. Aggregation and fractal aggregates. World Scientific, Singapore, 120 p.

Katz, A. J. and Thompson, A. H., 1985. Fractal sandstone pores: implications for conductivity and pore formation. Phys. Rev. Lett. 54 (12):1325.

Kaye, B. H., 1989. Image analysis techniques for characterizing fractal surfaces, in "The Fractal Approach to Heterogeneous Chemistry," (D. Avnir, ed.). John Wiley & Sons, pp. 55-66.

Krohn, C. E., 1988a. Fractal measurements of sandstones, shales, and carbonates. J. Geophys. Res. 93(B4):3297-3305.

Krohn, C. E., 1988b. Sandstone fractal and Euclidean pore volume distributions. J. Geophys. Res. 93(B4):3286-3296.

Krohn, C. E. and Thompson, A. H., 1986. Fractal sandstone pores: automated measurements using scanning-electron-microscope images. Phys. Review 33 (B9):6366-6374.

Langford, S. C., Zhenyi, M. and Dickinson, J. T., 1989. Photon emission as a probe of chaotic processes accompanying fracture. J. Mater. Res. 4(5):1272-1279.

La Pointe, P. R., 1988. A method to characterize fracture density and connectivity through fractal geometry. Int. J. Rock Mech. Min. Sci. & Geomech. Abstr. 25(6): 421-429.

Lovejoy, S. and Schertzer, D., 1991. Multifractal analysis techniques and the rain and cloud fields from 10^{-3} to 10^{6} m. Non-Linear Variability in Geophysics (D. Schertzer and S. Lovejoy, eds), Kluwer Academic Publishers: 111-144.

Mandelbrot, B. B., 1975. Les objets fractals: forme, hasard et dimension. Paris: Flammarion.

Mandelbrot, B. B., 1982. The Fractal Geometry of Nature. W. H. Freeman and Co., San Francisco, 460 p. (Revised edition of Fractals: Form, Chance and Dimension, Freeman and Co., San Francisco, 1977).

Mandelbrot, B. B., Passoja, D. E., and Paullay, A. J., 1984. Fractal character of fracture surfaces of metals. Nature 308:721-722.

Martin, J. E. and Hurd, A. J., 1987. Scattering from fractals. J. Appl. Cryst. 20:61-78.

Matsushita, M. and Ouchi, S., 1989. On the self-affinity of various curves, Physica D 38:246-251.

Meakin, P., 1991. Fractal aggregates in geophysics. Rev. Geophys. 29:317-354.

Mecholsky, J. J. and Mackin, T. J., 1988. Fractal analysis of fracture in Ocala chert. J. Mater. Sci. Let. 7:1145-1147.

Miller, S. M., McWilliams, P. C., and Kerkering, J. C., 1990. Ambiguities in estimating fractal dimensions of rock fracture surfaces. Rock Mechanics: Contributions and Challenges (Hustrulid and Johnson, eds.), Balkema, Rotterdam.

Nolte, D. D., Pyrak-Nolte, L. J., and Cook, N. G. W., 1989. The fractal geometry of flow paths in natural fractures in rock and the approach to percolation. Pure and Applied Geophys. 131 (1/2):111-138.

Norton, D. and Sorenson, S., 1989. Variations in geometric measures of topographic surfaces underlain by fractured granitic plutons. Pure and Applied Geoph. 131 (1/2):77-97.

Okuba, P. G. and Aki, K., 1987. Fractal geometry in the San Andreas Fault System. J. Geophys. Res. 92 (B1): 345-355.

Pande, C. S. and Richards, L. R., 1987. Fractal characteristics of fractured surfaces. J. Materials Sciences Letters 6: 295-297.

Peitgen, H. O. and Saupe, D. (eds.), 1988. The Science of Fractal Images. Springer Verlag.

Pfeifer, P. and Avnir, D., 1983. Chemistry in noninteger dimensions between two and three. I. Fractal theory of heterogeneous surfaces. J. Chem. Phys. 79 (7):3558-3565.

Pfeifer, P. and Obert, M., 1989. Fractals: basic concepts and terminology, IN "The Fractal Approach to Heterogeneous Chemistry" (D. Avnir, ed.). John Wiley and Sons, pp. 11-44.

Pfeifer, P., Obert, M., and Cole, M. W., 1989. Fractal BET and FHH theories of adsorption: a comparative study, in "Fractals in the Natural Sciences" (M. Fleischmann, D. J. Tildesley, and R. C. Ball, eds.). Royal Society of London, pp. 169-188.

Power, W. L. and Tullis, T. E., 1991. Euclidean and fractal models for the description of rock surface roughness. J. Geophys. Res. 96(B1): 415-424.

Pyrak-Nolte, L. J., Myer, L. R., Cook, N. G. W., and Witherspoon, P. A., 1987. Hydraulic and mechanical properties of natural fractures in low permeability rock. Proc. Int. Congress Rock Mech., Montreal, Canada, (G. Herget and S. Vongpaisal, eds.) pp. 225-231.

Richardson, L. F., 1961. The problem of contiguity: an appendix of statistics of deadly quarrels. General Systems Yearbook 6: 139-188.

Rieu, M. and Sposito, G., 1991a. Fractal fragmentation, soil porosity, and soil water properties: I. Theory. Soil Sci. Soc. Am. J. 55:1231-1238.

Rieu, M. and Sposito, G., 1991b. Fractal fragmentation, soil porosity, and soil water properties: II. Applications. Soil Sci. Soc. Am. J. 55:1239-1244.

Ruffet, C., Gueguen, Y. and Darot, M., 1991. Complex conductivity measurements and fractal nature of porosity. Geophysics 56 (6):758-768.

Russo, D. and Jury, W. A., 1988a. A theoretical study of the estimation of the correlation scale in spatially variable fields: 1. stationary fields. Water Resources Res. 23 (7):1257-1268.

Russo, D. and Jury, W. A., 1988b. A theoretical study of the estimation of the correlation scale in spatially variable fields: 2. nonstationary fields. Water Resources Res. 23 (7):1269-1279.

Sander, L. M., 1985. Growth by particle aggregation, in "Scaling Phenomena in Disordered Systems"(R. Pynn and A. Skjeltorp, eds.). NATA ASI Series, Plenum Press, New York, pp. 31-47.

Schlueter, E. M., Zimmerman, R. W., Cook, N. G. W., and Witherspoon, P. A., 1991. Fractal dimensions of pores in sedimentary rocks and relationship to permeability. LBL report #LBL-30853.

Schmidt, P. W., 1989. Use of scattering to determine the fractal dimension, Ch. 2.2 in "The Fractal Approach to Heterogeneous Chemistry" (D. Avnir, ed.). John Wiley and Sons, pp. 67-79.

Scholz, C. H. and Aviles, C. A., 1986. The fractal geometry of faults and faulting, in "Earthquake Source Mechanics" (S. Das, J. Boatwright, and C. H. Scholz, eds.). Monogr. 37, Amer. Geophys. Union, Washington D.C., pp. 147-155.

Snow, R. S., 1989. Fractal sinuosity of stream channels. Pure and Applied Geophys. 131 (1/2):99-109.

Sreenivasan, K. R., Prasad, R. R., Meneveau, C. and Ramshankar, R., 1989. The fractal geometry of interfaces and the multifractal distribution of dissipation in fully turbulent flows. Pure and Applied Geophys. 131 (1/2): 43-60.

Thompson, A. H., 1991. Fractals in rock physics. Annu. Rev. Earth Planet. Sciences 19:237-62.

Toledo, P. G., Novy, R. A., Davis, H. T. and Scriven, L. E., 1990. Hydraulic conductivity of porous media at low water content. Soil Sci. Soc. Am. J. 54:673-679.

Turcotte, D. L., 1989. Fractals in geology and geophysics. Pure and Applied Geophys. 131 (1/2):171-196.

Tyler, S. W. and Wheatcraft, S. W., 1989. Application of fractal mathematics to soil water retention estimation. Soil Sci. Soc. Am. J. 53(4):987-996.

Underwood, E. E. and Banerji, K., 1986. Fractals in Fractography. Materials Science and Eng. 80:1-14.

Van Damme, H., 1989. Flow and interfacial instabilities in Newtonian and colloidal fluids, in "The Fractal Approach to Heterogeneous Chemistry" (D. Avnir, ed.). John Wiley & Sons, pp. 199-225.

Wang, J. S. Y., Narasimhan, T. N., and Scholz, C. H., 1988. Aperture correlation of a fractal fracture. J. Geophys. Research 93(B3):2216-2224. novaculite

LAWRENCE BERKELEY LABORATORY
UNIVERSITY OF CALIFORNIA
INFORMATION RESOURCES DEPARTMENT
BERKELEY, CALIFORNIA 94720